Innovative Trend Analyses

5

Abstract

Innovative trend analysis is the most modern, simple, easy to interpret, and effective trend analysis procedure that incorporates first visual inspection for identification of the trend type whether increasing, decreasing, or no trend cases and then provide numerical calculation for the trend slope again by a very simple formulation. All the classical trend determination methodologies try to find holistic monotonic trend either over the whole record period or on pieces of subperiods. However, the innovative trend method compares last parts of any desired duration record length with earlier perions within the time series itself, hence, one can appreciate the trend variation within the record itself. Another innovative trend method is based on the number of crossings along the trend line, which should have the maximum number of crossing. This procedure helps to identify also the surplus and deficit parts of a given time series with respect to the trend line.

Keywords

Crossing · Innovative · Over-whitening · Simulation · Slope · Intercept

5.1 General

There are commonly used trend identification techniques such as Mann–Kendall (MK) and Spearman's Rho (SR) tests as explained in Chap. 3, but their validity is possible under a set of restrictive assumptions such as independent structure of the time series, normality of the distribution and length of data. It is also not possible to calculate trend magnitude (slope) except through regression approach, which brings additional assumptions for the theoretical validation in practical applications.

Z. Şen, *Innovative Trend Methodologies in Science and Engineering*,
DOI 10.1007/978-3-319-52338-5_5

Recent hydrologic regime changes due to potential climate variability impacts brought into focus the search for effective trend identification analysis. Numerous works in different parts of the world showed quasi-periodic natural behavior and systematic trends of key climate variables due to climate change and/or climate variability (Chap. 6). It is well known that changing climate is expected to have notable impacts on the rainfall–runoff processes due to increasing or decreasing trends in hydro-meteorological time series (floods, droughts, heat waves, etc.). These impacts can no longer be assumed to be stationary, which means that future replicates are no more statistically indistinguishable from the historical counterparts. If climate change is not taken into account then such changes or variability can lead to underestimation/overestimation of parameters for the design and operation of water infrastructures, water shortages, water stresses, and agricultural failures. Although some test procedures are presented for trend identification, there are restrictive assumptions with respect to serial structure (ignorance of correlation coefficient), normal probability distribution function (PDF) of the variables and rather lengthy datasets.

Two commonly used trend tests are Mann–Kendall (Mann 1945; Kendall 1975) test and Spearman's Rho test to the data set (Sen 1978). In many studies, these two nonparametric rank-based statistical tests are used for detecting monotonic trends in a given time series. The power of these tests has not been well documented but the simulation results by Yue et al. (2002a, b, c) indicate that the power depends on the pre-assigned significance level, magnitude of trend, sample size, and the amount of variation within a time series. That is, the bigger the absolute magnitude of trend, the more powerful are the tests; as the sample size increases, the tests become more powerful; and as the amount of variation increases within a time series, the power of the tests decrease. When a trend is present, the power is also dependent on the PDF type and the skewness coefficient. The simulation results also demonstrate that these two tests have similar power in detecting a monotonic trend, to the point of being indistinguishable in practice.

In the past, time series were often assumed as stationary or weakly stationary stochastic processes for simulation purposes. Due to anthropogenic (human disturbance) effects on climate, environment, drainage basin and atmosphere, such an assumption is not valid anymore. However, this is almost the case with economic time series. This implies that future predictions cannot be regarded as statistically indistinguishable from the past records. Current anthropogenic impacts substantially affect natural, environmental and economic variables. For instance, events as droughts, floods, and streamflow discharges are also influenced by climate impacts. Monotonic and steadily increasing trends in past records lead to the alteration of planning, operation and management practices of atmospheric researchers, meteorologists, climatologists, economics, and hydrologists alike. Therefore, prior to any future predictions, it is necessary to try and identify possible monotonic trend components in any given time series. Trend identification analyses have been extensively employed in natural works (Kalra et al. 2008; Miller and Piechota 2008; McCabe and Wolock 2002; Lins and Slack 1999; Douglas et al. 2000; Lettenmaier et al. 1994; Groisman et al. 2001).

This section presents preliminary results and applications of two effective and potential innovative trend identification methodologies that do not require many of the restrictive assumptions. The first one is concerned with the plot of a set of subseries from the original time series on a Cartesian coordinate system, where 45° straight-line implies no trend but any plot appearance above (below) this line implies increasing (decreasing) trends. The same methodology is capable to provide trend magnitude (slope) calculation. The other one, crossing trend analysis, depends on the crossing number of a given time series at the arithmetic average truncation level.

5.2 Probability Distribution-Statistical Parameter Trend Implications

The most important trend or shift component indicator in any time series is the PDF provided that there is a long series of available data that can be divided into at least two nonoverlapping equal parts. The frequency distribution function (or histogram) for each part is than fitted to a theoretical PDF and the comparison of these two PDFs provide first a visual inspection about the possibility of trend or sudden shift (jump) component. For the sake of explanation herein the theoretical PDFs are assumed as a normal PDF. Comparison of the relative position of these two PDFs to each other leads to seven different cases The first case is shown in Fig. 5.1 where

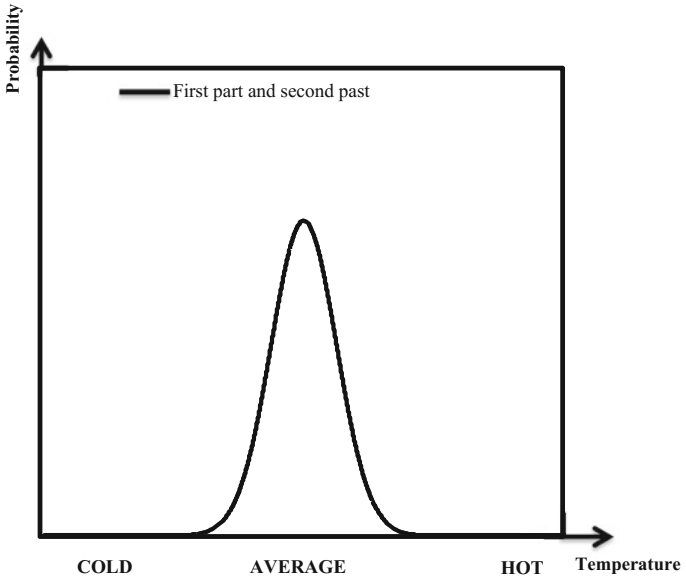

Fig. 5.1 No trend PDF

the two PDFs of the first and next half of the available time series record fall on each other then there is no trend component within the time series (Fig. 5.1). The property implies also that the time series is strictly stationary, because all the statistical parameters are constant along the time series. If one interprets this graph under the light of recent climate change she/he can state that there is no climate change and "hot," "mild," and "cold" climate states remain almost the same by time. Notice that for climate change interpretation the horizontal axis is taken as representative of temperature records.

As in Fig. 5.2 if there is a shift of the first part (past records) PDF toward higher values then there is the possibility of either an increasing trend or a jump that maybe sudden or over a very short period of time. One can decide qualitatively by visual inspection of the time series graph whether it is a trend or a jump. If the increase in the time series values toward recent values seems as gradual then one can conclude that there is an increasing trend, otherwise it is a jump. An important point at this point is that the time difference between the two PDFs in Fig. 5.2 is equal to the half duration time of the time series record duration. This last statement implies that in case of a trend there is a gradual increase from the statistical parameters of the first half toward the second half. This is a very important scrap of information, which enables one to calculate any parameters change slope by taking the difference between the two parameters and its division by the half duration.

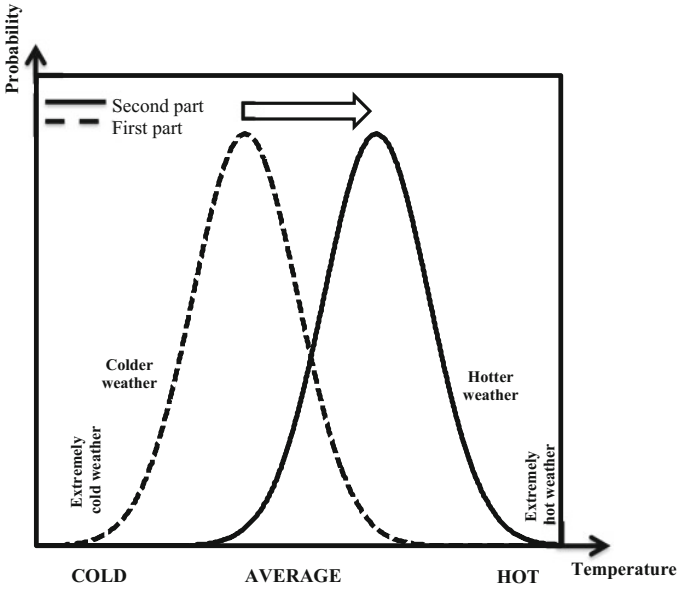

Fig. 5.2 Increase trend PDFs

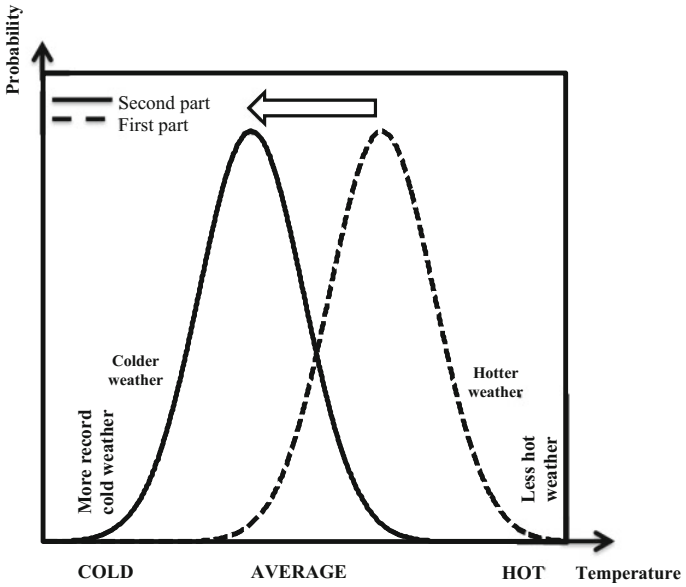

Fig. 5.3 Decreasing trend

In Fig. 5.2 by taking into consideration that the horizontal axis is for temperature records then one can make climate change implication interpretations as "colder," "extremely cold," "hotter," and "extremely hot" weather conditions. The reader may have his/her interpretations.

Decreasing trend or downward jump possibilities are shown in Fig. 5.3 on the basis of two-halves PDFs. The shift in the first part PDF is toward lower data values. Similar to the previous case the statistical parameters are decreased and the slope values can be calculated for each statistical parameter.

The previous graphs collectively imply that although there are changes in the arithmetic average values, but the standard deviation remains the same, i.e., homoscedasticity exists. These three figures are the fundamental assumption in the classical trend determination, because all the linear trend lines do not take into consideration possible changes in the standard deviation.

However, there may also be variations in the standard deviations, which can be identified by the comparison of the two parts' PDFs. The change in the variance, which is also valid for the standard deviation, is referred to as the variability in this book. For instance, the case in Fig. 5.4 an increasing variability is valid, because although there is no change in the arithmetic average the standard deviation has increased again during the half duration of the time series record length. Since, as a general rule, the area under any PDF is equal to one, expansion in this figure implies reduction in the peak value probability. As in the previous cases, the reader may emerge with his/her own interpretation by considering that the horizontal axis is for temperature records.

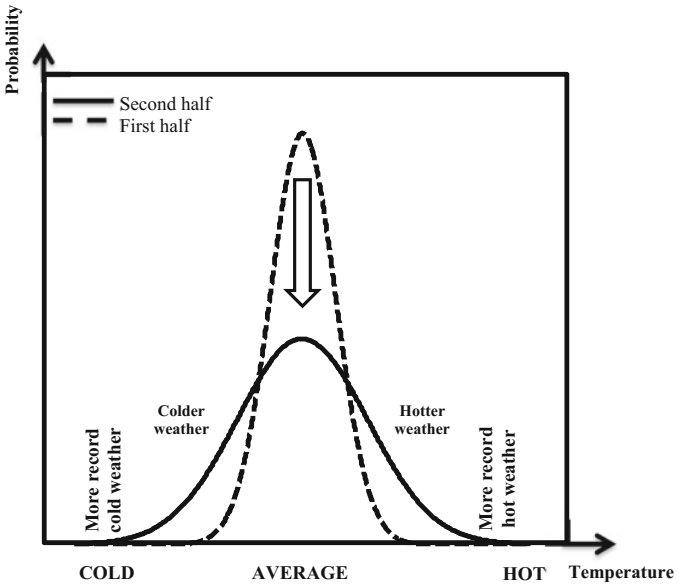

Fig. 5.4 Increasing variability

Opposite of increasing variability Fig. 5.5 is the representative of the decreasing variability. The comparison of the two PDFs indicates that the recent half records had shrinkage in the PDF, which is the reduction in the standard deviation. If after visual inspection of the time series graph one come out with gradual decrease in the standard deviation values then there is a standard deviation trend of which the slope is equal to the difference between the standard deviations divided by the half time series duration.

Figures 5.4 and 5.5 also imply that the underlying time series are first order stationary, because the arithmetic averages remain the same. More detailed information and methodological explanations are presented about the variability in Chap. 7.

It is also possible to have trend and also variability in the same time series, which is the case in some of the natural and environmental time series records. For instance, if one considers the relative positions of the first and second half PDFs as in Fig. 5.6, then s/he can conclude that there is changes in the arithmetic average and in the standard deviation simultaneously.

After all what have been explained about the relative positions of the first and second half PDFs, the reader must have got used to the interpretation. Anyone can interpretate that Fig. 5.7 represents

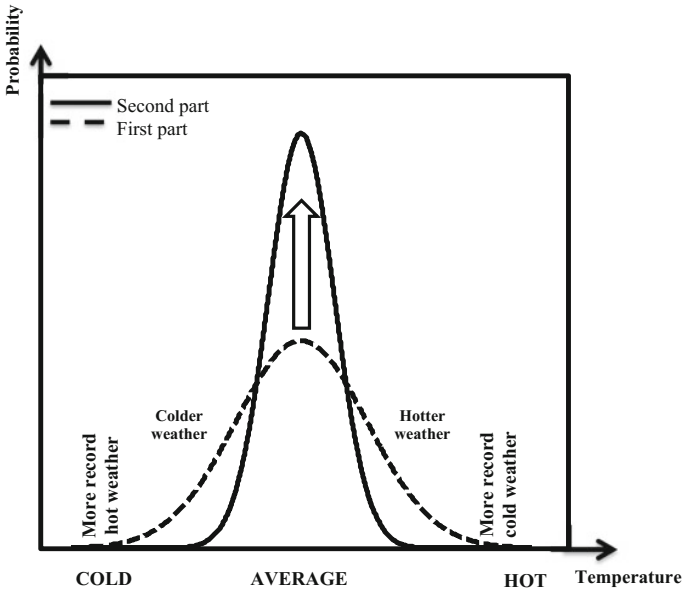

Fig. 5.5 Decreasing variability

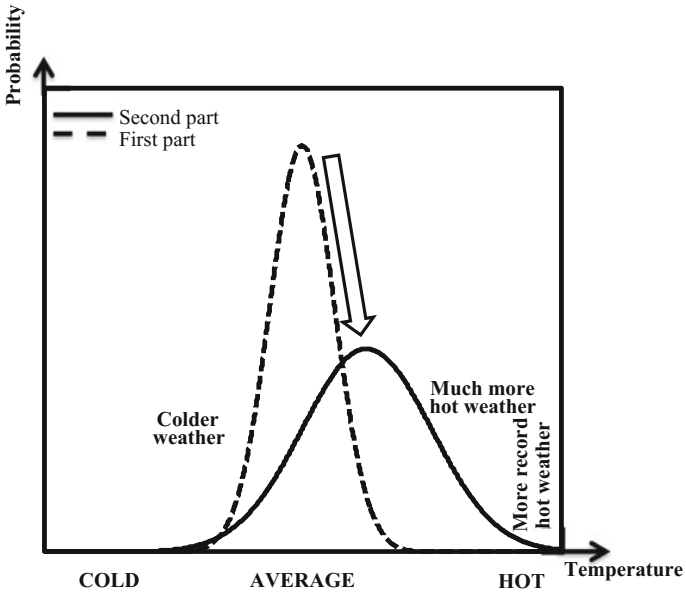

Fig. 5.6 Increasing trend and increasing variability

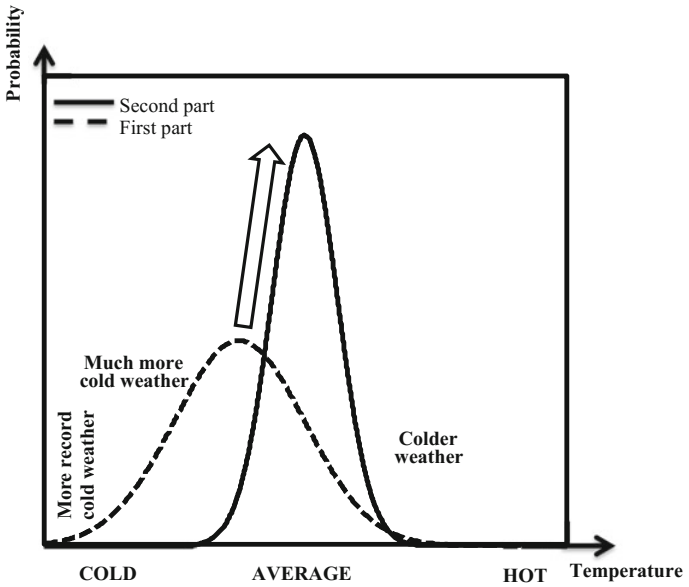

Fig. 5.7 Increasing trend and decreasing variability

5.3 Innovative Trend Identification Methodologies

In the following sequel, the innovative trend identification method presents as a new approach on the basis of subsection time series plots derived from a given time series on a Cartesian coordinate system. In such a plot trend-free time series subsections appear along the 1:1 (45°) straight-line. Increasing (decreasing) trends occupy upper (lower) triangular areas of the square area defined by the variation domain of the variable concerned. The validity of this new approach is documented through a set of Monte Carlo simulations by taking into consideration independent and dependent processes (Sect. 5.3). In this new approach, assumptions for the MK and Spearman's rho (SR) tests are avoided and additionally it is possible to calculate trend magnitude from square area plots.

The basis of the approach rests on the fact that if two time series are identical to each other, their plot against each other shows scatter points along 1:1 (45°) straight-line on the Cartesian coordinate system as in Fig. 5.8a. In the figure, there are 25 data points, which come from a nonnormal PDF. Whatever the time series, whether trend free or with monotonic trends, all points fall on the 1:1 straight-line when plotted. There is no distinction whether the time series are nonnormally distributed, having small sample lengths or possess serial correlations. One important conclusion from Fig. 5.8a is that data values sort themselves in ascending (or descending) order along the 1:1 straight-line. This idea will also be used later in this section in the trend identification procedure.

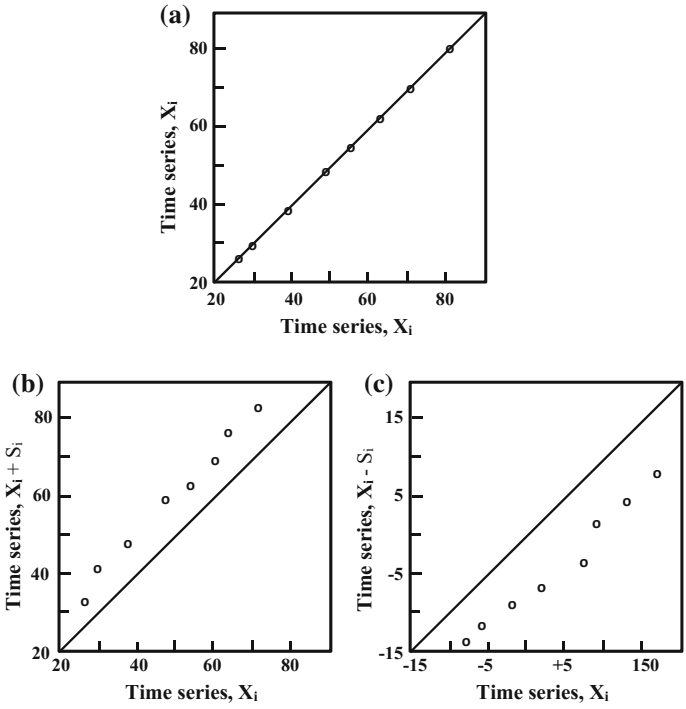

Fig. 5.8 **a** Trendless time series, **b** increasing trend, **c** decreasing trend

The same 25 data points are added with increasing and decreasing trends separately and then they are ordered and plotted against the original (trend-free) time series, which is also sorted in ascending order. The results are shown in Fig. 5.8b, c for increasing and decreasing trends, respectively. It is obvious that in the case of increasing (decreasing) monotonic trend, the scatter points fall above (below) the 1:1 straight-line. For any trial with nonnormal, small sample and serially correlated time series, similar scatter diagrams are obtained for increasing and decreasing trends.

The next question is how could one identify the existing trend in a given time series with respect to the idea of 1:1 straight-line? The answer appears as a plot of the first half of the same time series against the second half according to the above-mentioned idea. In Fig. 5.9a, b, the same time series as shown in Fig. 5.8b, c are used, this time by considering two-halves and the sorting procedure. It becomes obvious that monotone increasing (decreasing) trend in the given time series fall above (below) the 1:1 straight-line. This idea can be used for engineering, environmental, economic, or hydro-climatic time series trend identifications.

On the other hand, it is also possible to have time series with half plots similar to Fig. 5.9 as in Fig. 5.10, where there are scatter points on both sides of 1:1 straight-line. In Fig. 5.10a low (high) values are more (less) in the first half than the

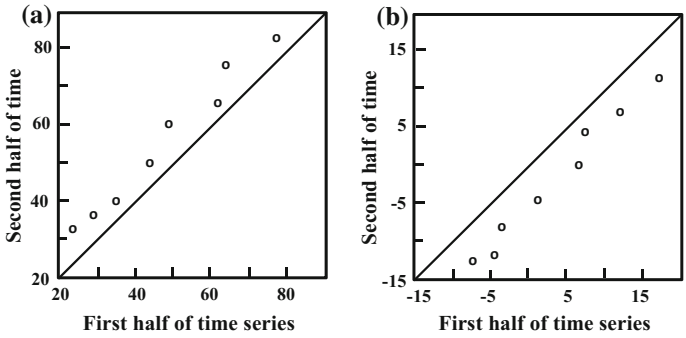

Fig. 5.9 Time series halves with monotonic trends, **a** increasing, **b** decreasing

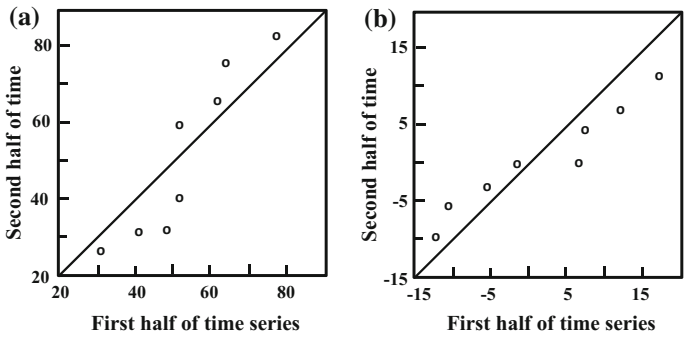

Fig. 5.10 Time series halves with nonmonotonic trends, **a** increasing, **b** decreasing

next half, whereas in Fig. 5.10b the opposite situation occurs. These cases correspond to nonmonotonic trends where within the same time series there are increasing and decreasing trends at different scales even hidden ones (Chap. 6).

In practical applications, a mixture of the all the cases explained in this section appears accordingly, the necessary interpretations can be done for better understanding the composition of the time series structure.

5.3.1 Application

The applications of the innovative trend methodology are presented for different annual runoff and rainfall series recorded at various locations in Turkey in addition to annual Danube river flows. Aslantas and Menzelet Dams are the catchment areas in southern Turkey on Ceyhan River that confluences into the Mediterranean Sea. Cizre streamflow station is on the Tigris River right at the border between Turkey and Iraq. Danube annual streamflow records are from Orshava station in Romania.

Figure 5.11a, b are from two hydrological catchments in Turkey, each reflecting annual flows from 1954 to 2003. For the interpretation of these figures, it is better to think of the annual flows in three clusters as "low," "middle," and "high" flows. In order to make a detailed interpretation, the scatter diagram on 1:1 straight-line graphs are divided into three verbal clusters as "Low," "Medium," and "High." In Fig. 5.11a, "low" flows represent points on the increasing trend upper triangle, which means that there is an increase in the "low" flows during the second half of the historic record (1979–2003) with respect to the first half (1954–1978). In the "medium" cluster, there is almost no trend, and finally, the "high" cluster indicates decreasing trend. All these explanations imply that the annual flow series have a composition of various trend patterns.

The annual flow scatter diagram between two-halves of Menzelet station are shown in Fig. 5.11b, where the "low" flows have slight increasing component within the "low" flow cluster small and big values. The "medium" flow cluster is

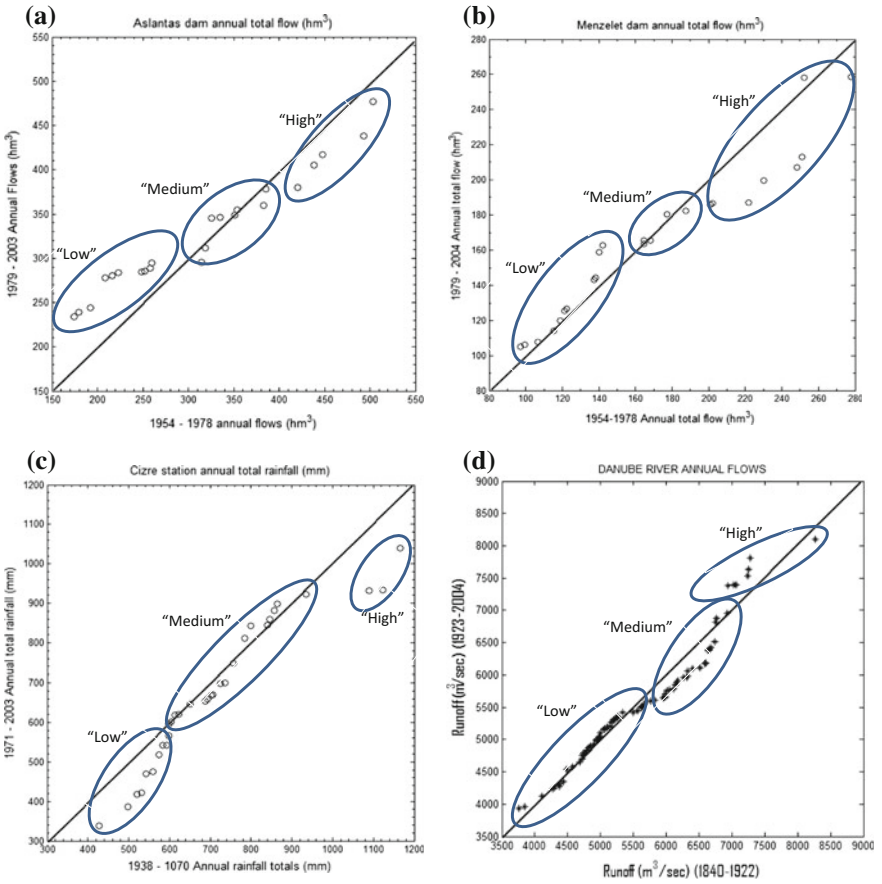

Fig. 5.11 Various 1:1 plots. **a** Aslantas Dam. **b** Menzelet Dam. **c** Cizre Station. **e** Danube River

trend free because the scatter of points concentrate closely around 1:1 straight-line. In the "high" cluster a decreasing trend component is valid. At this station there is a decrease in the "high" flow values; and hence, in the future, water stress is more likely to appear.

In Fig. 5.11c, "low" and "high" clusters indicate decreasing trends, whereas the "medium" cluster is trend free. Comparatively "high" flow trends have shorter duration than in the "low" cluster portion. Most of the duration is occupied by "medium" cluster flows with no significant trend component. Furthermore, the "low" and "high" flows have decreases in the (1971–2003) duration compared to (1938–1970). This also gives the warning that at this station droughts and floods are bound to increase in the future.

Finally, Danube river annual flows do not have any significant trend in the "low" flow cluster, which includes all the annual flows less than about 5750 m^3/s (Fig. 5.11d). "Medium" flows have some decreasing trend and "high" flow cluster has slightly significant increasing level.

Based on the above explanations, the following important points can be summarized about the innovative trend methodology.

(1) If scatter points on the first quadrant of the Cartesian coordinate system fall on another straight-line parallel to 1:1 straight-line, then there is a monotonic increasing (decreasing) trend depending on the fall of the scatter points onto the upper (lower) triangular area of the scatter region,
(2) The closer the scatter points are to the 1:1 straight-line, the weaker the trend magnitude (slope),
(3) In the case of nonmonotonic trends (i.e., composition of various trends in the time series), the scatter points take their positions on a curve.

This innovative trend method does not require restrictive valid assumptions whatever the sample size, serial correlation structure of the time series, and non-normal PDFs.

5.4 Innovative Trend Simulation

Trend analyses occupy a significant role in the climate change studies since almost four decades. It is significant to try and identify monotonic trends in a given time series so as to make future predictions about the possible consequences on the urban environment, economics, water resources, agriculture, environmental, and many other socioeconomic aspects of the life. Although there are now classically accepted and frequently used trend tests in the open literature such as MK trend analysis and SR test, they are based on some restrictive assumptions as normality, serial independence, and rather long sample sizes. Besides they search for a single monotonic trend without any specification such as "low," "medium," and "high" values, which may have different trend patterns. Many time series records have

serial dependence and, therefore, it is very helpful to provide a methodology, which is not affected from such restriction. It is the main purpose of this section to provide simulation results and applications of an earlier innovative trend analysis methodology based on the 1:1 (45°) straight-line comparison of the scatter points on a Cartesian coordinate system.

Natural and human activities affect different processes in a continuous manner and their impacts appear in the forms of trends or sudden jumps. Some particular natural phenomena such as El Niño, as well as all kinds of large scale water resources development projects, may alter hydrological processes and may lead to abrupt changes in the hydrological time series (Xiong and Guo 2004). The presence of deterministic trends in the time series may provide information about the future evolution of the process or at least on the possible modifications. In practical applications, the knowledge of the trend for a given variable of interest may help to forecast future realizations and to design future scenarios. Nowadays, with the growing importance of climate change assessment, trend detection, and evaluation are subjects of intensive scientific research (Brunetti et al. 2001; Burn et al. 2002; Kahya and Kalaycı 2004; Groisman et al. 2004; Cohn and Lins 2005; Barbosa et al. 2008), as also testified in the recent fourth assessment report of the Intergovernmental Panel on Climate Change (IPCC 2007). One branch of climate change science is devoted to analyzing the past climate events and inside this branch trend detection and statistical significance testing assume an important role (Trenberth 2007).

Natural and man–made effects are defined as the long-term behavior of concerned variables on the average, which provides distinctive features for future behaviors of the same variable. During the last four decades, the most sought such behavior is the possibility of monotonic trend existence in a given time series, because the current day change impacts and causative decisions require gradual increasing or decreasing trends. Especially, time series records are searched for two reasons; the first one is trend identification, and then its magnitude determination as reflection of the "increasing" or "decreasing" quantities. Although there are trend identification methods, which provide answers for the existence of trends, but the magnitude is measured either by linear regression approach (Hirsh and Slack 1984; Lettenmaier et al. 1984) or through the median slope calculation according to Sen (1978) procedure. This estimator is robust to the effect of outliers in the series. It has been widely used to compute trends in hydro-meteorological series (Wang and Zhou 2005; Zhang et al. 2001).

None of the classical trend tests such as the MK test takes into account classical parametric and most commonly used serial correlation and, hence, they require independence structure in the applications. In general, independence test can be carried out mainly by examining the autocorrelation coefficients of the time series. If the absolute values of the autocorrelation coefficients for a time series consisting of n observations are not larger than the typical critical value, i.e., $1.96/\sqrt{n}$ corresponding to the 5% significance level (Douglas et al. 2000), then the observations in this time series can be accepted as being independent from each other. The

significance of the trend is determined using Kendall's test because it does not assume an underlying probability distribution function (PDF) of the data series.

The main purpose of this section is to present extensive computer simulation for robust trend identification procedure as already proposed by Şen (2012), which is not dependent on any restrictive assumption as serial correlation, nonnormality, and sample number. The procedure is based on the plot of time series two-halves against each other after sorting in ascending order. This procedure helps to identify trends distinctively in the low, medium, and high values also. The difference of this section lies in its extensive independent process and dependent first order Markov process simulation results, which indicate the relationship between the trend slopes and first order serial correlation coefficient. Additionally, the comparisons of this trend procedure with the classical methodologies including MK and SR trend statistics and Sen's trend slope are given in table form with necessary interpretations.

5.4.1 Fundamental Methodology

As mentioned in Sect. 5.3, a new trend analysis methodology by Şen (2012) depends on the 1:1 (45°) straight-line on a Cartesian coordinate system, where it corresponds to trend-free case and any deviation from this line indicates trend existence and the closer is the plots to 1:1 (45°) straight-line, the smaller is the trend slope.

In the innovative trend identification methodologies as explained in Sect. 5.3 upper and lower triangular areas correspond to trend existence. Figure 5.12 is prepared as the plot of sorted time series versus two trend-embedded synthetic time series. Each series is obtained by adding a linear monotonic increasing and decreasing trend into the original time series in the upper and lower graphs of Fig. 5.12. In the middle square, plots versus trend-free time series are given after sorting in ascending order. The final product yields the fact that the upper (lower) triangular area includes increasing (decreasing) trends, respectively. Additionally, on the 1:1 straight-line plots, increasing trend time series points can be interpreted by considering low and high values subjectively in two groups. Hence, since low values are concentrated near the 1:1 straight-line, the trend existence is weaker than the group of high values, which significantly deviate from the straight-line 1:1 straight-line. On the other hand, in the lower triangular area, the time series have low values' cluster, this time away from the line, whereas high values approach the 1:1 straight-line implying comparatively weaker trend existence in the structure of the time series considered all based on visualization.

In Fig. 5.13, previous increasing and decreasing trend time series are plotted within themselves by having the whole series first into two and then sorting them in ascending order. The result is increasing (decreasing) trend in the time series according to their complete structure. This point provides a new way of trend assessment, which takes into account not only the ranks (nonparametrically) but also the measurements parametrically.

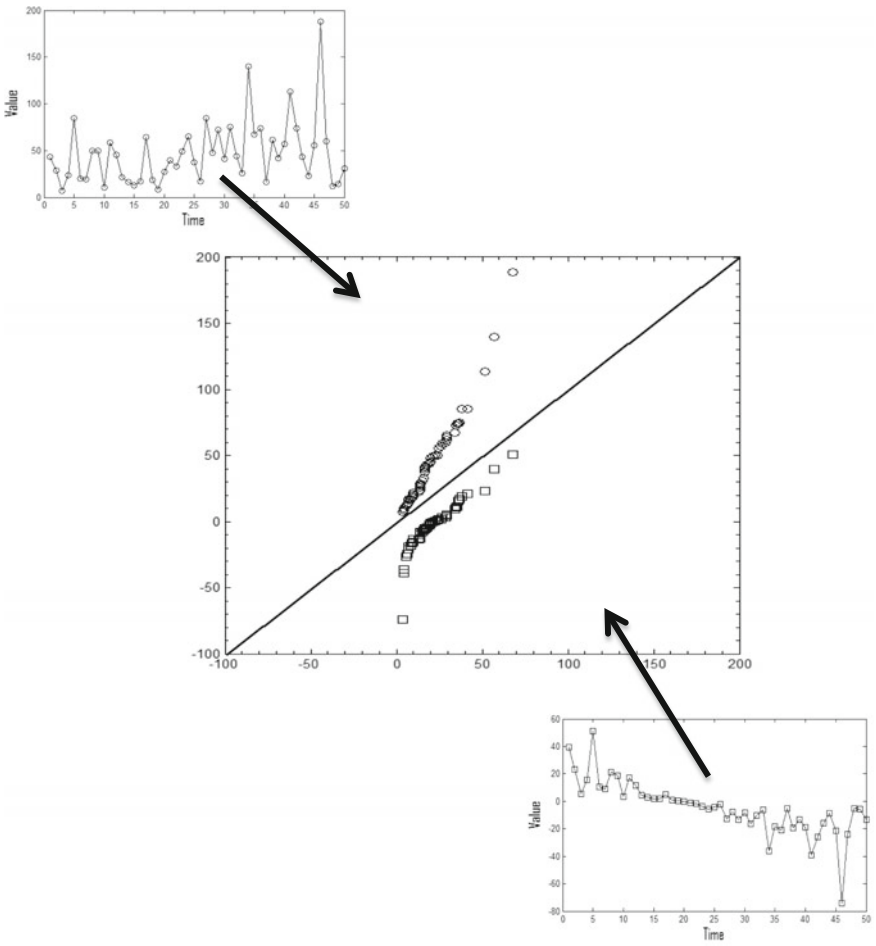

Fig. 5.12 Decreasing and increasing trends versus trend-free time series

In the following sections, extensive simulation study is performed for the validity of the innovative trend methodology by use of independent and dependent processes.

5.4.1.1 Simulation Methodology

There are different aspects in time series analyses depending on the purpose, which may take shape according to needs in any planning, design, and operation and maintenance stages. The prime goal is to deduce some useful and objective information for future works that support final decisions. Initially, Hazen (1914) was interested in extending the past records to future predictions and for this purpose he designed a very simple pre-computer era procedure by writing each one of the past records on separate paper pieces, mixed them thoroughly in a bag and

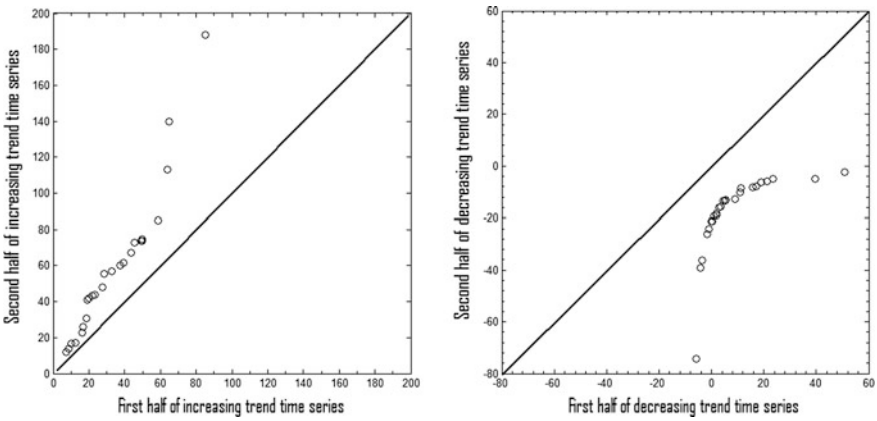

Fig. 5.13 Half time series

then drew one by one for future time series construction. This primitive procedure had the assumptions of almost trend-free synthetic time series with the same statistical similarity to past time series. The only difference was in the sequence of past record values. With the appearance of digital computers in 1950s, stochastic processes became in use for the analysis of historical records with the purpose of constructing their future replicates synthetically in such a way that statistical properties are indistinguishable from the historical records (Şen 1974). Autoregressive (AR) and autoregressive integrated moving average (ARIMA) models in various degrees of order become in use in many disciplines including hydrology for water resources planning, operation, and management stages (Box and Jenkins 1970; Montanari et al. 1997).

Figure 5.12 can be used as a template to identify trend existence in a given time series. For this purpose, the square area template in the first quadrant can be thought in three portions. These are enumerated below:

(1) The main diagonal, 1:1 (45°) straight-line presents no trend line,
(2) The upper right angle triangular area is for increasing trends,
(3) The lower right angle triangular area is for decreasing trends.

These points will be explained by simulation studies based on dependent and independent process, trend free and trend-embedded time series in addition to practical applications. Theoretically, in case of exactly the same two time series, there is no areal scatter on the coordinate system but the scatter is along the 1:1 straight-line only. This means that each time series is its own reflection on the 1:1 straight-line (see Fig. 5.8a), which corresponds to trend free case, whereas upper (lower) triangular area is for increasing (decreasing) trends. Figure 5.14a presents 30 points from stochastic processes, where all the points are aligned along the 1:1 straight-line in a random scatter manner similar to Fig. 5.8a. Figure 5.14b presents

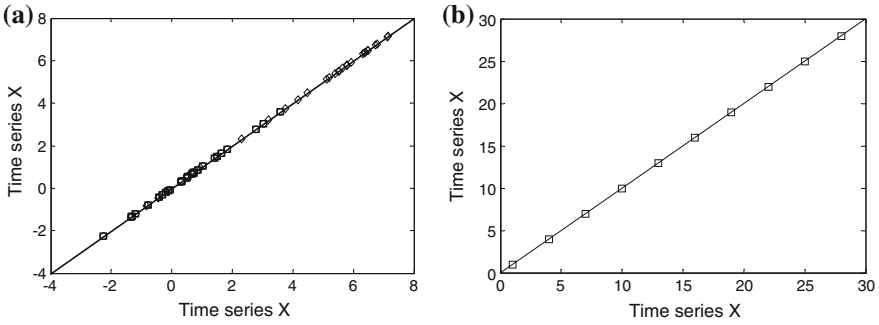

Fig. 5.14 **a** Stochastic time series (o independent; ◦ dependent), **b** regular time series

time series with regular (deterministic) increments. Such plots have the following results:

(1) Time series own reflections appear along the main diagonal (1:1 straight-line) scatter irrespective of trend or trend-free serial structure,
(2) Whatever the PDF of the time series, the end plot also appear along the same diagonal,
(3) Serial correlation of the time series does not play any role in such plots,
(4) Seasonality component also does not affect the appearance along the main diagonal scatter,
(5) The number of sample has not role and again the plots appear along the 1:1 (45°) straight-line.

After all these points, the main question is whether such plots may help to identify trend (or trends) in a given time series?

This question brings to mind similar to plot of a given time series versus itself, what happens when the first half of the series is plotted against its second half time series? For this purpose, the same time series maybe fragmented into mutual and successive half subseries. A very significant clue from Figs. 5.13 and 5.14 is that along the main diagonal the points are sorted according to ascending order automatically. This point gives the idea of sorting the two-halves into ascending orders and then to plot the first half versus the next on the Cartesian coordinate system. This opens the door to compare "low" ("medium," "high") values with "low" ("medium," "high") values of the two-halves.

In order to explain some of the main points in the innovative trend methodology, first of all, trend-free independent (normal or non-normal) processes are generated with zero mean and unit standard deviation, which is then embedded with a sequence of monotonic trends by considering a set of trend slopes, d, (−0.009:0.002:0.009). The length of the generated synthetic sequence is adapted as 10,000, which is then divided into two-halves of 5,000 elements each. Inspiration

from the above explanations gives rise to the following significant points for the application of the methodolog:

(1) Generate a set of trend-embedded sequences and divide them into two-halves,
(2) Sort each half in ascending order,
(3) Plot the first half against the second half on the square area (on the Cartesian coordinate system).

Figure 5.12 is the end product of such a procedure with different time series and their signatures on the square area, which leads to the following inferences:

(1) Trend-free halves plot appears along the 1:1 (45°) straight-line,
(2) Increasing (decreasing) trends are within the upper (lower) triangle of the square area,
(3) They are all in the forms of straight-lines parallel to each other with 45° slope, which implies that the trend slope, d, in the original series does not have any effect on these straight-lines,
(4) As the trend slope, d, in a time series increases, corresponding straight-line plot appearances on the square area get away from the trend-free line (main diagonal, 1:1 or 45° line),
(5) Positive and negative trend slopes have reflective effects with reference to no trend (1:1 straight-line).

These points indicate that the innovative trend identification methodology does not give information only about the existence of the trend in the time series but additionally about its magnitude (slope, d). The significant conclusion is that any plot of two-halves from a given time series in ascending order is enough to identify trend existence and its magnitude irrespective of data length. In Fig. 5.15, although trends are taken from respective 10,000 length time series, just for the sake of clarity and explanation only 1,000 points are shown. In each one of these time series increasing and decreasing monotonic trends are shown explicitly with their corresponding consequences on the square area.

5.4.1.2 Dependent Process Simulation Results

In order to perform the power of the proposed methodology, a set of Monte Carlo simulations are presented by taking into consideration first order (Markov) autoregressive (AR) stochastic process with PDFs. The simulation procedure first generates synthetic time series, X_i, of length 10,000 values according to the following model:

$$X_i = \mu + \rho(X_{i-1} - \mu) + \sigma\sqrt{(1-\rho^2}\varepsilon_i, \tag{5.1}$$

where μ and σ are the mean and standard deviation of the process; ρ is the first order serial correlation coefficient and ε_i is the normal independent process with zero mean and unit variance, NIP (0, 1). The set of simulations is based on the serial

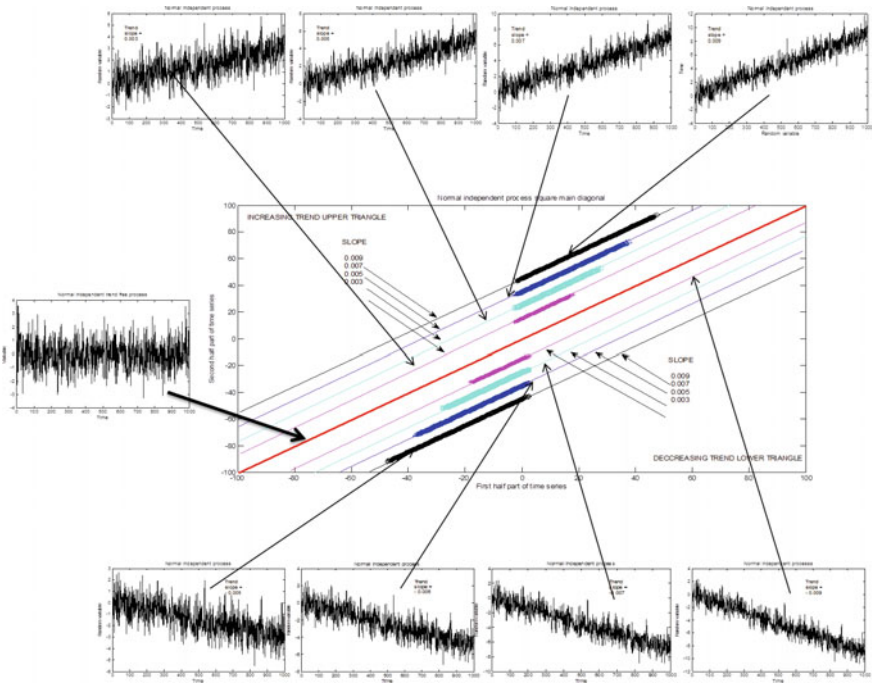

Fig. 5.15 Independent process trends on square area

correlation coefficients, $\rho = 0.1\ (\pm 0.2) \pm 0.9$. Equation (5.1) generates trend-free stationary time series, which are converted to nonstationary forms by embedded with increasing and decreasing trend components of slopes, $d = 0.001\ (\pm 0.02) \pm 0.09$. The slope is embedded through the simple linear trend component addition to the basic stochastic process according to $X_i + d_i$, where $i = 1, 2, \ldots, 10{,}000$.

Figure 5.16 summarizes the simulation results from above-mentioned AR process given a high serial correlation coefficient, $\rho = 0.9$, with a set of embedded trends. Each one of the thick lines includes 5,000 generated normal dependent values (because 10,000 values were generated for each simulation) as the first half versus the second half. The fine lines are drawn through these thick simulation results in each triangular area. It is obvious that as the absolute value of the trend slope increases the results fall away from the 1:1 straight-line. During the simulation, it is noted that the straight-lines in Fig. 5.16 are a result of normal PDF.

Comparison of Figs. 5.15 and 5.16 indicate that whether the time series is independent or dependent, there is no difference in the square area procedure and as long as the basic time series has a monotonic trend, the appearance of the two-halves sorted magnitude plots will appear along 45° straight-lines without any distinction. This statement alleviates the drawback of the MK trend test, which requires independent data. Additional illuminating points can be drawn from the

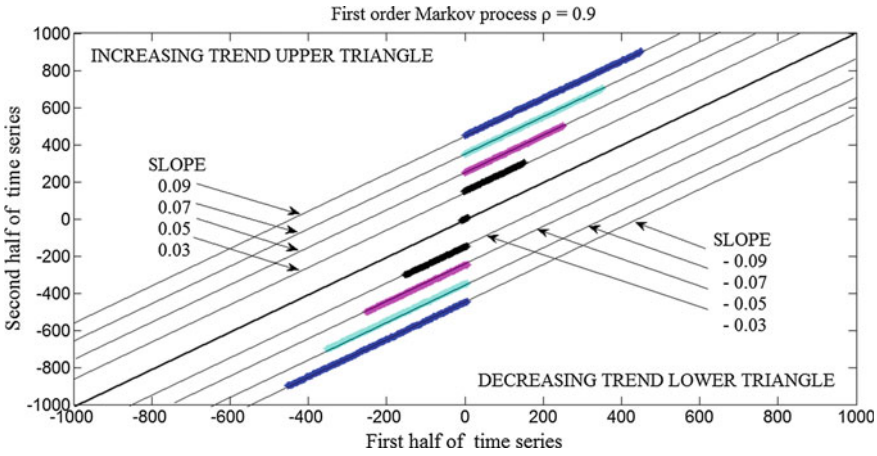

Fig. 5.16 Trend lines with respect to 1:1 straight-line for a set of slopes

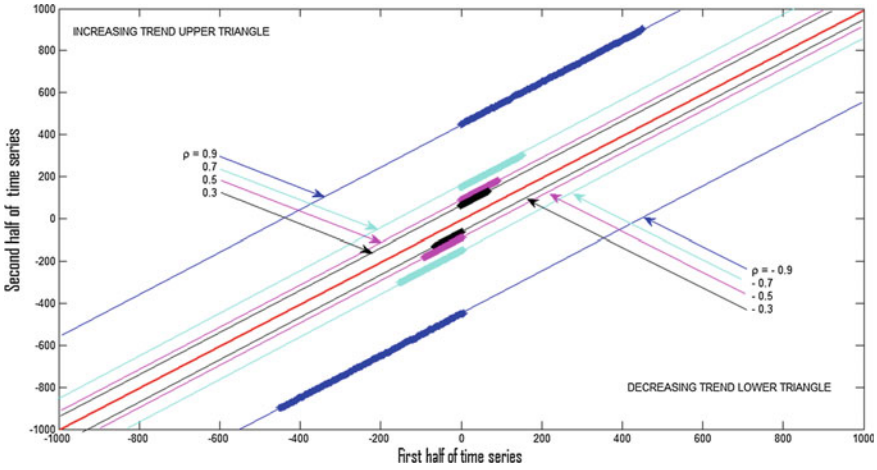

Fig. 5.17 Trend chart of trend (d = 0.009) embedded first order AR processes

square area plot in Fig. 5.17, where this time the trend slope is kept constant (d = 0.009) and trend appearances are shown for a set of serial correlation coefficients (−0.9; −0.7; −0.5; −0.3; 0.0; 0.3; 0.5; 0.7; 0.9).

This figure indicates that the upper (lower) triangle include positive (negative) correlation coefficient cases, which is another improvement on the MK test, where the serial correlation cannot be accounted at all in the calculations. The more the serial correlation coefficient absolute value, at the same trend magnitude (herein, d = 0.009), the more effective is its occurrence on the square area template.

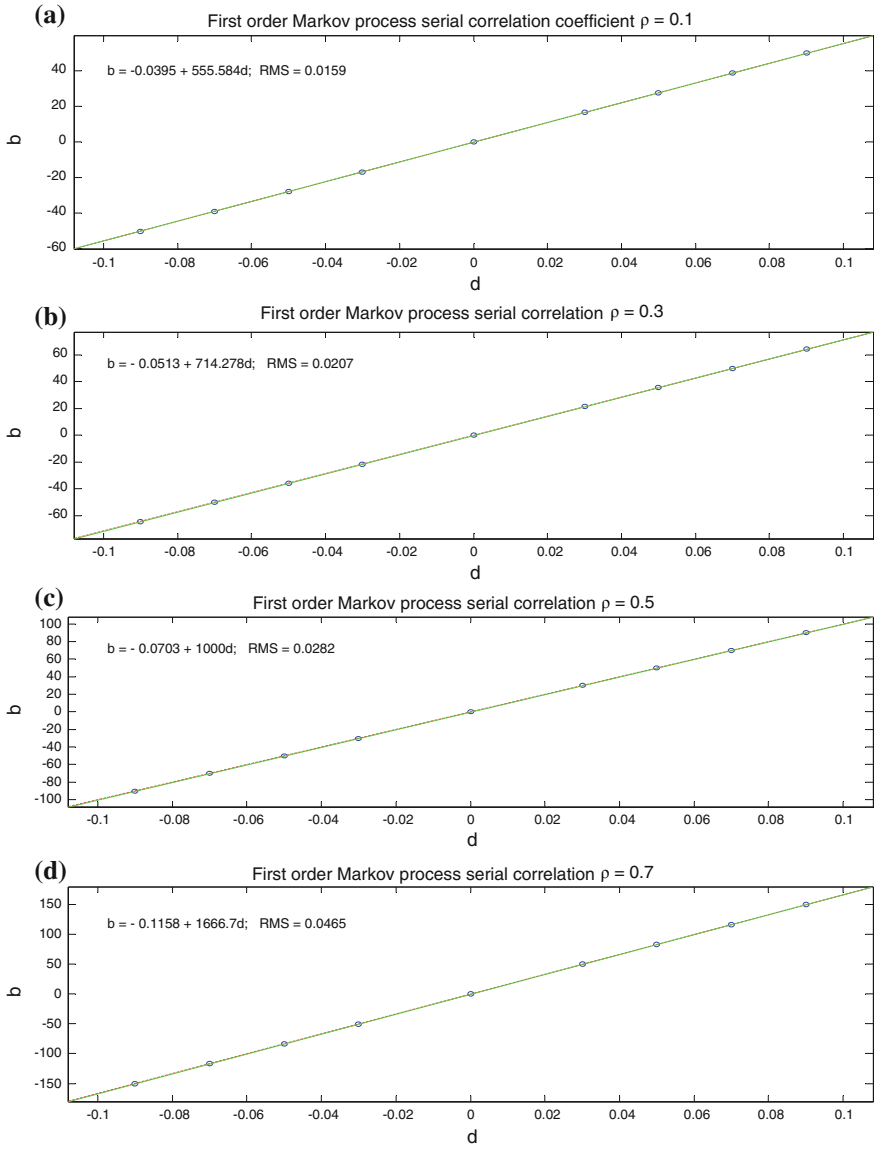

Fig. 5.18 Trend magnitude square area plot slope relationship for **a** $\rho = 0.1$; **b** $\rho = 0.3$; **c** $\rho = 0.5$; $\rho = 0.7$

Figure 5.18 provides linear relationship between the trend and square area template slopes for given serial correlation coefficient. In the same figure corresponding root mean square (RMS) errors are also presented and they are all very small within practically acceptable limits.

Table 5.1 Trend slope, serial correlation coefficient and trend line intersection

Trend slope, d	Independent process	First order stochastic serial correlation coefficient (ρ)				
	0.0	0.1	0.3	0.5	0.7	0.9
−0.09	−45	−50.048	−64.343	−90.080	−150.133	−450
−0.07	−35	−38.934	−50.058	−70.080	−116.800	−350
−0.05	−25	−27.824	−35.772	−50.080	−83.465	−250
−0.03	−15	−16.713	−21.486	−30.078	−50.131	−150
0.00	0.0	0.0	0.0	0.0	0.0	0.0
+0.03	15	16.624	21.372	29.920	49.871	150
+0.05	25	27.736	35.658	49.921	83.205	250
+0.07	35	38.846	49.944	69.922	116.538	350
+0.09	45	49.957	64.223	89.922	149.872	450

It is obvious that there is almost perfect linear relationship between the trend magnitude (slope, d) and the trend representative line on square area template for any given serial correlation coefficient. Table 5.1 provides numerical values of the relationship between ρ, d, and b.

This table can be used to determine the magnitude of monotonic trend in any time series provided that the serial correlation coefficient and the slope on the square area template are determined.

After all what have been explained above, it is possible to state that the new methodology yields information about the low values of the first half with low values of the second half leading to the following conclusions:

(1) If low, high, medium, and high value plots of the two-halves are above (below) the 1:1 (45°) straight-line, then there is an increasing or decreasing trend,
(2) In case of increasing (decreasing) trend, if all the low, medium, and high values fall on almost parallel line to 1:1 (45°) straight-line then there is a single monotonic trend in the time series,
(3) Otherwise, low, medium, and high values may have different positions on the plot area, and this implies to the existence of various sub-trends in the time series structure,
(4) The proposed methodology can provide detailed information about the low, medium, and high value trends in the time series and their relative effectiveness to each half.

In Fig. 5.19, a set of trend-embedded (d = 0.009) simulation synthetic sequences is given, for a set of autocorrelation coefficients.

The corresponding plots of these time series around 1:1 (45°) straight-line are given in Fig. 5.20 for various serial correlation coefficient. Again straight-lines parallel to 1:1 (45°) and basic line are plotted based on half time series simulation result values (5,000 values) according to sorting procedure. Since embedded trends

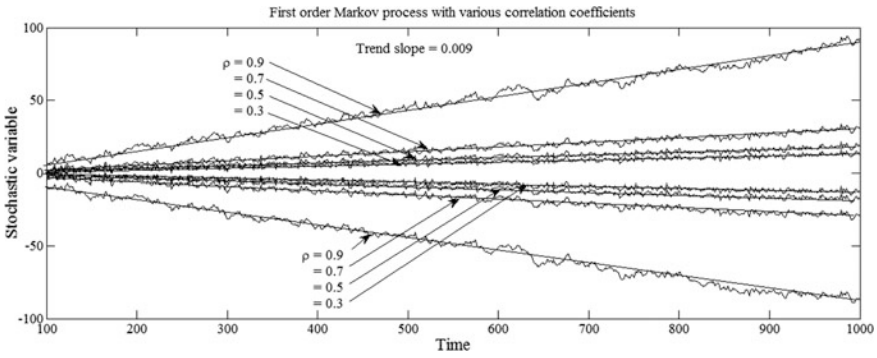

Fig. 5.19 Increasing and decreasing trends

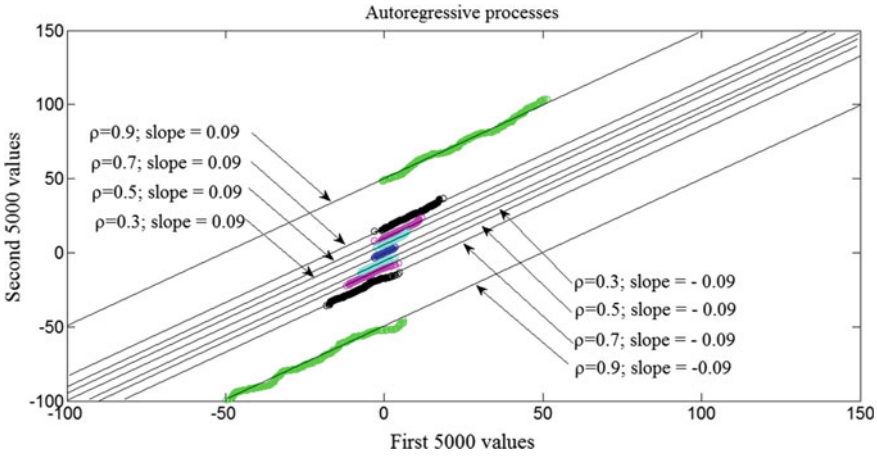

Fig. 5.20 Trend lines (0.09) with respect to 1:1 line for a set of correlation coefficient

are monotonic, the lines are parallel to 1:1 (45°) straight-line. One can conclude from this figure that as the absolute value of the serial correlation coefficient increases the trend representing lines get away from 1:1 (45°) straight-line basic line. The chart in this figure helps to answer to the following questions:

(1) Is there a linear trend embedded in the given time series?
(2) What is the serial dependence coefficient (ρ) in the series?
(3) Is it possible to identify the trend in a given series without pre-whitening?

Figure 5.21 represents comparatively weaker (d = 0.009) trend for the same set of serial correlation coefficients. There is no change in the previous interpretations and the straight-lines get away from the basic 1:1 line.

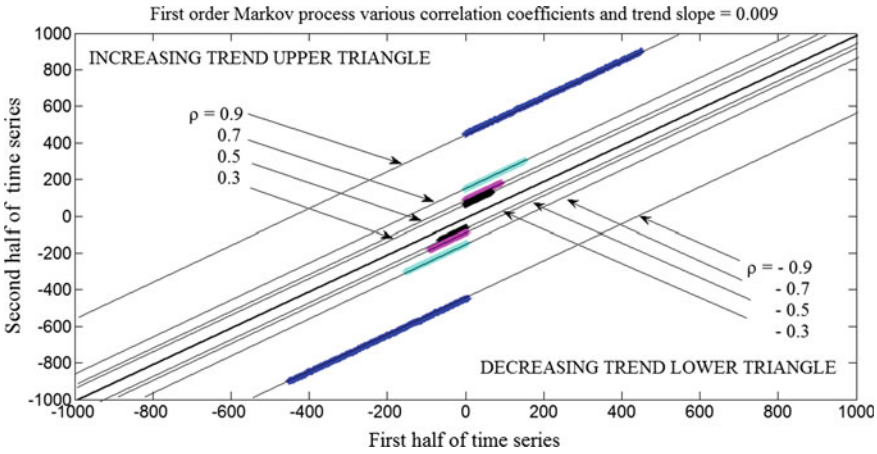

Fig. 5.21 Trend lines (d = 0.009) with respect to 1:1 (45°) straight-line for a set of correlation coefficient

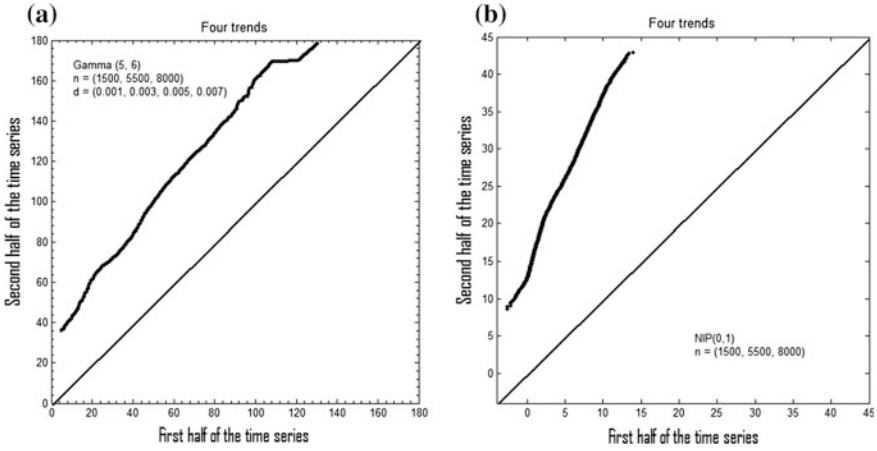

Fig. 5.22 Nonmonotonic trends, **a** Gamma PDF. **b** Normal independent process

All the previous figures had monotonic trends as in Fig. 5.21, but to expand the applicability of the proposed 1:1 (45°) straight-line methodology. Figure 5.22 is given as a representative example among numerous simulation results that increasing but nonmonotonic trends can also be depicted by the same methodology.

In Fig. 5.22a, Gamma PDF simulation results are presented with shape and scale parameters as 5 and 6, respectively. Four different but successive trends are embedded onto the basic time series, where the first, second, third, and fourth trend components appear between 1–1,500; 1,501–5,500; 5,501–8,000; and 8,001–10,000, and trend slopes are 0.001; 0.003; 0.005; and 0.007, respectively. The same

simulation is repeated for normal independent process, NIP (0, 1), in Fig. 5.7. One can deduct from Fig. 5.22 the following points:

(1) Even though the PDF is Gaussian the final trend plots in Fig. 5.22b does not appear along a straight-line parallel to 1:1 (45°) straight-line contrary to Figs. 5.20, 5.21, 5.22a,b and 5.31 where only monotonic trends exist,
(2) The 1:1 (45°) straight-line methodology is capable of identifying increasing but nonmonotonic (multiple) trends. This provides a possibility even to identify hidden (short duration) sub-trends in the whole time series,
(3) In the case of more than one successive trend, the plots according to 1:1 (45°) straight-line method appear on the upper (piecewise increasing) and lower (piecewise decreasing) triangular areas as curvature (nonlinear) traces,
(4) Combination of monotonic and piecewise trend embedded time series performances mentioned above, lead to deduction that any nonparallel line implies a combination of various scale nonmonotonic trends in the same time series.

There will not be any uncertainty of a trend estimate under few extreme minimum/maximum values, because the procedure in this section singles them out on the 1:1 (45°) straight-line plot domain. However, in conventional trend identifications, especially regression line fitting to a given time series will be affected by the extreme values. In case of small sample size of a time series, again since each couple of points from two-halves appears without any influence on other points on the scatter diagram in Fig. 5.22, the possible trend component will show itself.

5.5 Innovative Trend Significance Test

Time series might embed characteristics of past changes concerning climate variability in terms of shifts, cyclic fluctuations, and more significantly in the form of trends. Identification of such features from the available records is one of the prime tasks of hydrologists, climatologists, applied statisticians, or experts in related topics. Although there are different trend identification and significance tests in the literature, they require restrictive assumptions, which may not be existent in the structure of time series. In this section, a method is suggested with statistical significance test for trend identification in an innovative manner. This method has nonparametric basis without any restrictive assumption and its application is rather simple with the concept of subseries comparisons that are extracted from the main time series. The method provides privilege for selection of sub-temporal half periods for the comparison, and finally, generates trend on objective and quantitative manners. The necessary statistical equations are derived for innovative trend identification and statistical significance test application.

5.5.1 Deterministic Basis

In order to explain the basic idea behind the innovative methodology, first of all a linear trend function is considered between an independent time variable, t, and dependent variable, y, as,

$$y = a + bt \tag{5.2}$$

where a and b are the intercept on y axis and slope parameters, respectively. In a deterministic methodology, there are few alternatives to determine the parameter values.

(1) The simplest way is applicable provided that the independent, (t_1, t_2), and corresponding dependent, (y_1, y_2), variable pairs are known as two points. The substitution of these values into Eq. (5.2) helps to calculate the parameters from resulting two equations by elimination methodology,
(2) Calculation of the slope value, $b = (y_2 - y_1)/(t_2 - t_1)$, and its substation into Eq. (5.2) leaves only one unknown, which can then be calculated by substitution of coordinates either one of the given points leading to $a = y_1 - bt_1$ or $a = y_2 - bt_2$,
(3) If a regular sequence of n independent time variable, $(t_1, t_2, \ldots, t_n)$ and corresponding dependent variable sequence, $(y_1, y_2, \ldots, y_n)$ are given then one can calculate the unknown parameters, (a and b), either by considering any two points and apply the same methodology as in the two previous items or by consideration of all the given set of coordinates simultaneously through a linear regression methodology.

The core of the innovative trend test methodology is similar to this last item parameter calculation. The question is, provided that independent and dependent variable sequences are available, how to obtain the straight-line trend parameters? The explanation of this point can be given through the following deterministic numersimulation results are presented with shapeical example.

Let the parameter values in Eq. (5.2) be as $a = 2.5$ and $b = 0.25$ in addition to the number of data, say, $n = 126$. It is obvious that the result will appear as a straight-line given in Fig. 5.23a.

In Fig. 5.23b the innovative trend plot of the same deterministic data is presented as already explained by Şen (2012, 2014). In brief, the innovative trend plot requires division of the given time series into two-halves each sorted in ascending order, and finally, plot of the first half versus the second half as in Fig. 5.23b. In the preparation of this figure dependent variable sequence values, $(y_1, y_2, \ldots, y_n)$, are used for data line construction. The following features can be deduced from Fig. 5.23b.

(1) Deterministic dependent variable half plots fall on a definite straight-line referred to as "Data line,"

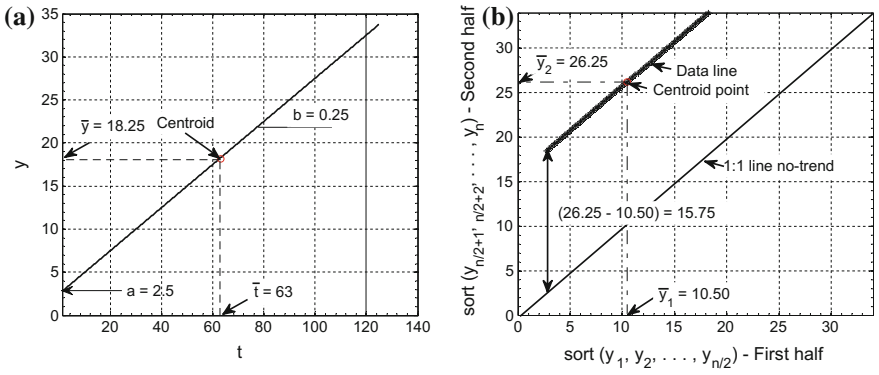

Fig. 5.23 Deterministic trend. **a** Data plot. **b** Innovative trend plot

(2) 1:1 (45°) straight-line indicates neutral trend (notrend) line and any deviation from this line indicates existence of a trend in the given dependent variable (Şen 2012). In Fig. 5.23b there is an obvious increasing trend because the data line is above the 1:1 (45°) straight-line,
(3) The arithmetic averages of the two-halves appear as the "Centroid point" that falls on the data line,
(4) The vertical difference between the data and 1:1 (45°) straight-lines is related to the slope of the existing trend in the dependent variable (Şen 2014),
(5) The vertical distance is equal to the difference between the arithmetic means of the two-halves, which appears as 15.57 in Fig. 5.23.

In the previous studies, there have not been any formulation derivations but qualitative assessments only. In this chapter, new numerical trend identification procedure and significance test are presented in the following sequel.

After the completion of above five steps one can calculate the slope, b, of the trend according to the following expression:

$$b = \frac{2(\bar{y}_2 - \bar{y}_1)}{n}, \tag{5.3}$$

where $\bar{y}_1$ and $\bar{y}_2$ are the arithmetic averages of the first and the second halves of the dependent variable, y, sequence, and n is the number of data. The substitution of the numerical values as $n = 126$, and the arithmetic averages from Fig. 5.23b as $\bar{y}_1 = 10.50$ and $\bar{y}_2 = 26.25$ into Eq. (5.3) yields $b = 0.25$, which is exactly the same value in Fig. 5.1. Hence, the procedure in the preparation of Fig. 5.23b with the use of Eq. (5.3) helps to find the slope of the trend in a given time series.

On the other hand, the calculation of y axis intercept, a, on the vertical axis in Fig. 5.23a, can be achieved according to the second item in the abovementioned parameter value calculations. For this purpose, one needs to know the coordinates of a single point, which is logically adapted as the arithmetic averages of time

sequence, $\bar{t}$, and, $\bar{y}$, of the dependent variables, respectively (Fig. 6.23a). The substitutions of these coordinate values and the slope from Eq. (5.3) into Eq. (5.2) gives the trend intercept parameter estimation as

$$a = \bar{y} - \frac{2(\bar{y}_2 - \bar{y}_1)}{n}\bar{t} = \bar{y} - b\bar{t}. \tag{5.4}$$

Finally, the substitution of the relevant quantities into the basic equation (Eq. 5.2) leads to the most detailed formulation of the innovative trend expression as

$$y = \bar{y} - \frac{2(\bar{y}_2 - \bar{y}_1)}{n}\bar{t} + \frac{2(\bar{y}_2 - \bar{y}_1)}{n}t = \bar{y} - b(\bar{t} - t). \tag{5.5}$$

In case of notrend, $\bar{y}_1 = \bar{y}_2$ and this last expression leads to $y = \bar{y}$, which means that the time series has a constant arithmetic average and, hence, no trend for which the innovative trend slope is 1:1 (45°) line as in Fig. 5.23b.

5.5.2 Stochastic Basis

In case of stochastic variables most often one has hydro-meteorological time series that require trend search for different purposes and most often for the climate change possibilities. In general, any hydro-meteorological time series has deterministic components as possible jumps, periodicities, and trends in addition to the stochastic residuals that are free of any deterministic parts. Herein, the identification of trend component is explained similar to the deterministic basis as explained in the previous subsection. In order to show the effectiveness of the proposed model, two synthetically generated time series are examined for the establishment of the stochastic basis of the innovative trend identification. The first example is for a normal probability distribution (PDF) and the second one is for a skewed Gamma type PDF.

5.5.2.1 Normally Distributed Stochastic Time Series

A synthetic time series is generated according to a first order Markov process with the mean, standard deviation and first order correlation coefficient values as μ = 10, σ = 5 and ρ = 0.5, respectively, with normal (Gaussian) PDF random component. The length of the stochastic time series is considered as n = 1,000 and synthetically a trend is embedded with slope b = 0.015. The generated synthetic time series with these specifications is presented in Fig. 5.24a. Generation of synthetic sequences with different serial correlation coefficients and their innovative trend plots fall on the same "Data line" within practically acceptable sampling relative errors of less that ±5%.

All the necessary quantitative values are provided on the innovative trend plot in Fig. 5.24b. The substitution of these mean values into Eq. (5.3) yields the slope

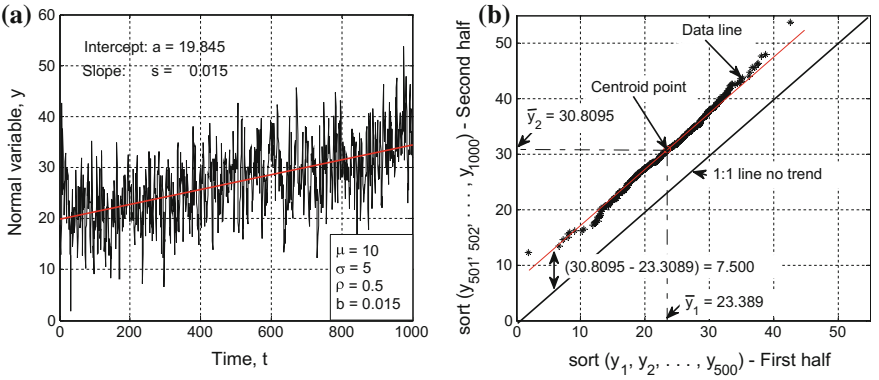

Fig. 5.24 Normal stochastic process **a** time series and trend, **b** innovative trend plot

value of the embedded trend as $s = 2(30.8095 - 23.389)/1000 = 0.0148 \cong 0.015$, which is the value of the embedded slope in the stochastic process.

The arithmetic averages of the time series independent time, t, and dependent, y, variables are $\bar{t} = 500$ and $\bar{y} = 27.159$, respectively. The corresponding intercept value can be obtained from Eq. (5.4) by substitution of the relevant values as $a = 27.159 - 0.0148 \times 500 = 19.76$, which is within less than $\pm 5\%$ relative error, r_e, from the value in Fig. 5.24a. Herein, $r_e = 100 \times (19.845 - 19.760)/19.845 = 0.42\% < 5\%$, and this value is within the acceptable limit of error.

5.5.2.2 Gamma Distributed Stochastic Time Series

In practical applications Gamma PDF is frequently used, because depending on the parameter values different PDF types appear. In the simulation, again $n = 1{,}000$ data set is generated as dependent variable, y, with the trend slope, $b = 0.020$, shape parameter, $\alpha = 2.3$, scale parameter, $\beta = 5.4$ and correlation coefficient, $\rho = 0.5$. The final result with trend component is presented in Fig. 5.25a, which is one of the samples from an ensemble of different 1,000 length synthetic series.

In order to calculate the slope value, all the necessary quantities are given in Fig. 5.25b. The substitution of the relevant quantities from Fig. 5.25b into Eq. (5.3) yields the slope value as $b = 2 \times (40.696 - 29.667)/1000 = 0.021$, which is within $\pm 5\%$ error limits from the slope value in Fig. 5.18a.

On the other hand, the time series time, t, and, y, variable averages are $\bar{t} = 5.4.3$ yields $a = 35.182 - 0.021 \times 500 = 24.682$. The relative difference between this value and the corresponding intercept in Fig. 5.18a is $100 \times (24.682 - 24.153)/24.682 = 2.14\%$, <10% and, therefore, these results remain within the sampling error limits.

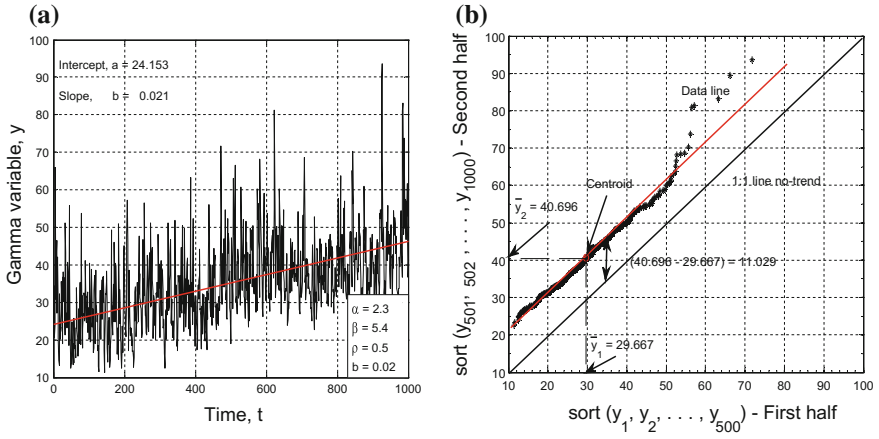

Fig. 5.25 Gamma stochastic process, **a** time series and trend, **b** innovative trend plot

5.5.3 Statistical Innovative Trend Test

The trend analysis as presented in this chapter is based on the comparison of two-half sample means. A test is convenient for the construction of confidence intervals by taking into consideration the difference between two population means. For this purpose, the null hypothesis, H_0, implies that there is not a significant trend if the calculated slope value, b, remains below a critical value, b_{cr}. Otherwise, an alternative hypothesis, H_a, is valid when $b > b_{cr}$. In order to develop an innovative significance test, it is necessary to derive the PDF of null hypothesis case. It is not necessary to search for the significance test of the intercept parameter, because the trend line is supposed to pass through the arithmetic averages of the independent and dependent variables. As for the slope parameter Eq. (5.3) shows that the stochastic property of b is a function of the first and second half time series arithmetic average values. Since $\bar{y}_1$ and $\bar{y}_2$ are also stochastic variables the first order moment (expectation) of the slope value can be obtained by taking the expectation of both sides leading to

$$E(b) = \frac{2}{n}[E(\bar{y}_2) - E(\bar{y}_1)]. \tag{5.6}$$

After all what have been explained in the previous sections in the case of no trend, the centroid point falls on the 1:1 line, which implies that $E(\bar{y}_1) = E(\bar{y}_2)$ and, therefore, $E(b) = 0$.

On the other hand, the variance of the slope can be calculated as $\sigma_b^2 = E(b^2) - E^2(b)$ or $\sigma_b^2 = E(b^2)$, which is equal to the second order moment of the

slope variable. This can be obtained by taking the expectation of both sides in Eq. (5.3) after the square operator resulting in

$$\sigma_b^2 = \frac{4}{n^2}\left[E\left(\overline{y}_2^2\right) - 2E(\overline{y}_2\overline{y}_1) + E\left(\overline{y}_1^2\right)\right].$$

Because $E\left(\overline{y}_2^2\right) = E\left(\overline{y}_1^2\right)$, it is possible to obtain the following expression:

$$\sigma_b^2 = \frac{8}{n^2}\left[E\left(\overline{y}_2^2\right) - E(\overline{y}_2\overline{y}_1)\right]. \tag{5.7}$$

The correlation coefficient between the two mean values is given in the stochastic processes as follows:

$$\rho_{\overline{y}_2\overline{y}_1} = \frac{E(\overline{y}_2\overline{y}_1) - E(\overline{y}_2)E(\overline{y}_1)}{\sigma_{\overline{y}_2}\sigma_{\overline{y}_1}}. \tag{5.8}$$

Substitution of the numerator of this expression into Eq. (5.7) and consideration stochastically that $\sigma_{\overline{y}_2} = \sigma_{\overline{y}_1} = \sigma/\sqrt{n}$ and, hence, Eq. (5.8) takes its final form as follows:

$$\sigma_b^2 = \frac{8}{n^2}\frac{\sigma^2}{n}(1 - \rho_{\overline{y}_2\overline{y}_1}). \tag{5.9}$$

In this last expression, $\rho_{\overline{y}_2\overline{y}_1}$ implies cross-correlation coefficient between the ascendingly sorted two-halves' arithmetic averages. The standard deviation of the sampling slope value can be obtained from Eq. (5.9) as

$$\sigma_b = \frac{2\sqrt{2}}{n\sqrt{n}}\sigma\sqrt{1 - \rho_{\overline{y}_1\overline{y}_2}}. \tag{5.10}$$

Furthermore, the third order moment of the slope variable is also equal to zero and the same is valid for all the odd order moments. This is the reason why the PDF of the slope, s, abides with the normal (Gaussian) PDF with zero mean and the standard deviation given in Eq. (5.10).

The most significant point in the application of this formulation is that the cross-correlation is between the two-sorted half time series. The statistical significance of the innovative trend slope test can be achieved through a normal (Gaussian) PDF with zero mean and standard deviation equal to Eq. (5.10).

5.5.4 Application

The stochastic innovative trend analysis as explained in the previous sections is applied to time series from different parts of the world. As for the long records

Table 5.2 Descriptive features of actual data

Name	Country	Record duration (year), n	Statistical features	
			Mean, $\overline{y}$	St. Dev., $\sigma_{\overline{y}}$
New Jersey	USA	116	53.04 °F	1.30 °F
Danube River	Romania	164	5566.8 m^3/s	944.91 m^3/s
Tigris River	Turkey	49	483.92 mm	124.74 mm

Southeastern New Jersey annual mean temperature data, Danube River annual discharge data, and annual mean precipitation data from the Tigris River drainage basin at Diyarbakir meteorology station are considered for the application to actual data. The simple statistical quantities of each station are presented in Table 5.2.

In general, most researchers look for the monotonic trend possibility within a given hydro-meteorological time series along the whole record length. The time series with trend and the innovative trend plots are given in Figs. 5.26, 5.27 and 5.28 for each data set.

In the application of innovative trend test, the basic criterion is the normal (Gaussian) PDF with zero mean and standard deviation σ_b (Eq. 5.10). If at α percent significance level the confidence limits of a standard normal PDF with zero mean and standard deviation is b_{cri} then the confidence limits (CL) of the trend slope can be expressed according to the following expression:

$$\text{CL}_{(1-\alpha)} = 0 \pm b_{\text{cri}}\,\sigma_b, \tag{5.11}$$

where σ_b is the slope standard deviation. All the necessary calculations and additional information with the operations in the last column are presented in Table 5.3.

One of the important points in this table is high cross-correlation values in row 6, because they are calculated depending on the ordered sequence in each half series. Slope value, b, of each station falls outside the lower and upper confidence limits and, therefore, in row 11 the alternative hypotheses, H_a, are adopted and they indicate the existence of trends (YES) as decisions. In the last row, the type of trend is stated depending on the slope sign in row 3.

The trend identification is one of the most significant elements in any climate change study. The most commonly used methodology for the identification is the Mann–Kendal (MK) trend test, but it requires few basic assumptions, which may not be valid in natural hydro-meteorological time series. MK test is misleading in the presence of data autocorrelation. Although several researchers have suggested pre-whitening procedure to render the original time series into a serially independent structure, but it is noticed that such a procedure cannot yield really embedded trend in the time series but with some bias. In the classical trend calculations serial independence, homoscedasticity and normal probability distribution assumptions must be satisfied. Such assumptions maybe guaranteed to a certain extent after

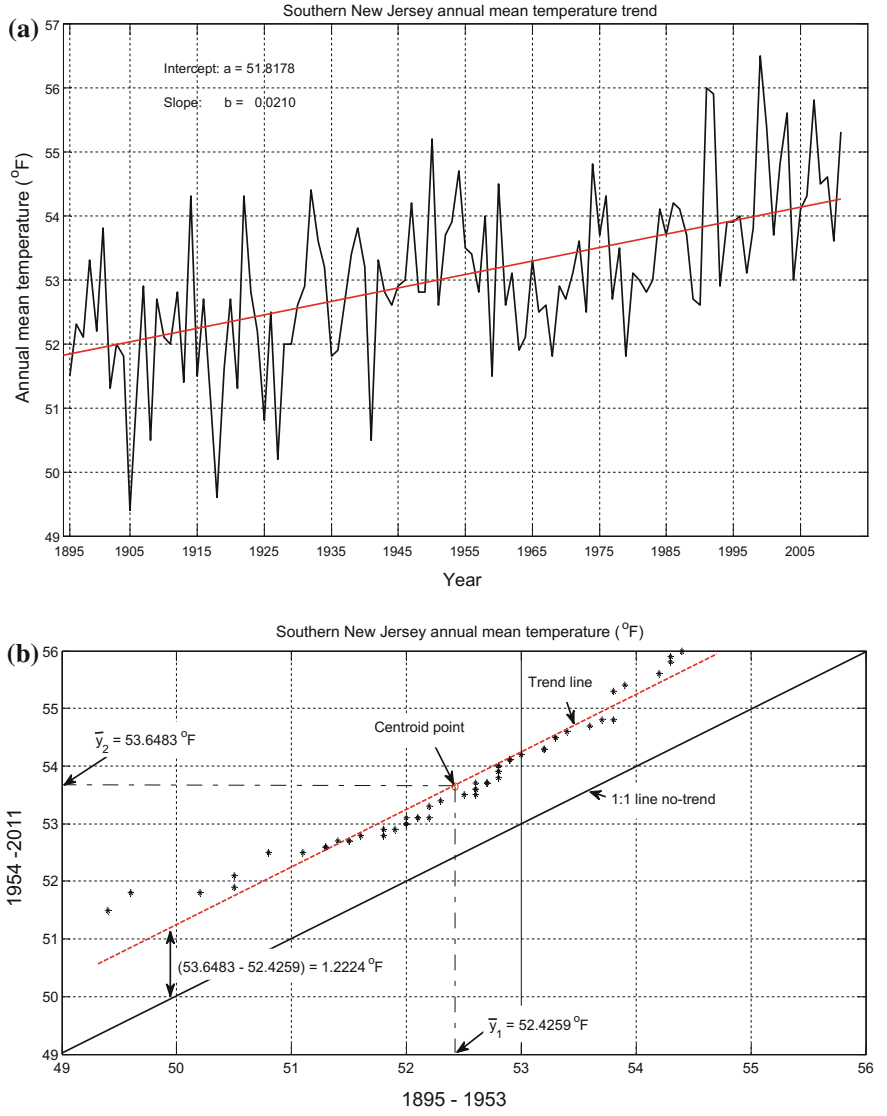

Fig. 5.26 Southern New Jersey annual mean temperature time series. **a** Time series and trend, **b** innovative trend plot

convenient transformations of the original series, which may not reflect genuine trend behavior of the series.

The procedure presented in this section does not require assumption, and it is based on the comparison of the two ascendingly ordered halves from the original

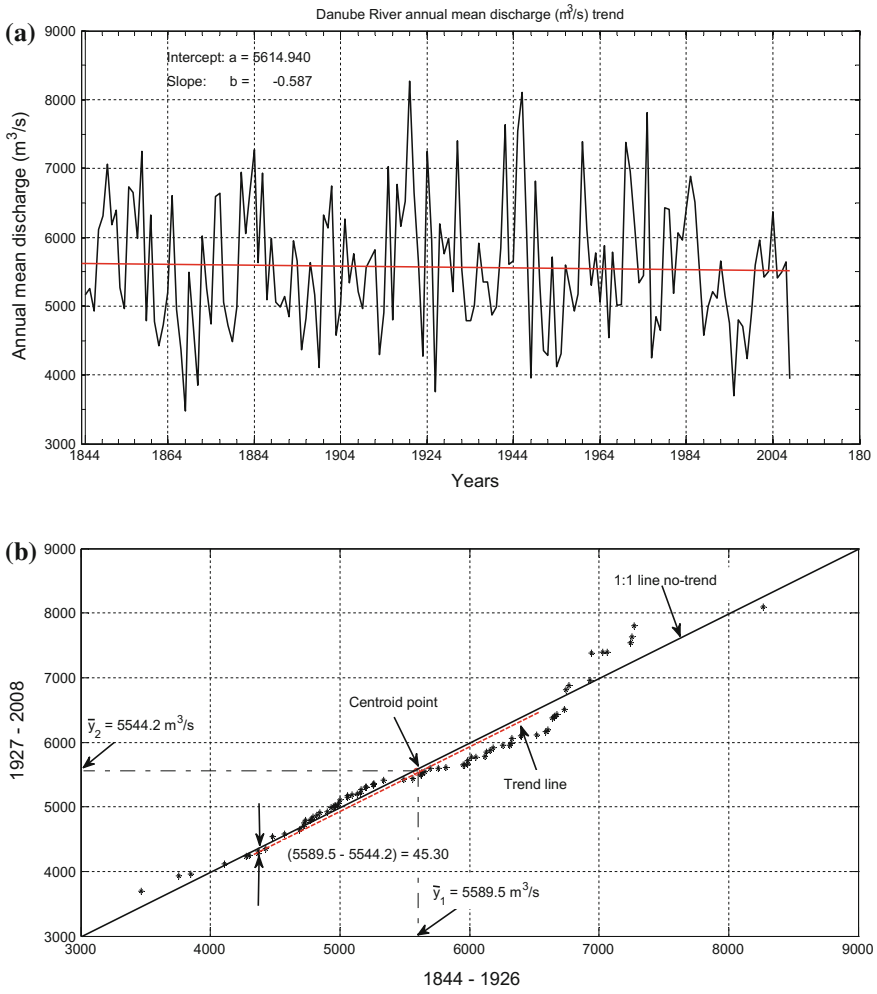

Fig. 5.27 Danube River annual mean discharge time series. **a** Time series and trend, **b** innovative trend plot

time series. The necessary formulations for the trend identification are derived explicitly and then monotonic trend significance test is presented in detail. The applications of the innovative trend significance statistical test are presented for the New Jersey temperature, Danube River discharge, and Tigris River meteorology

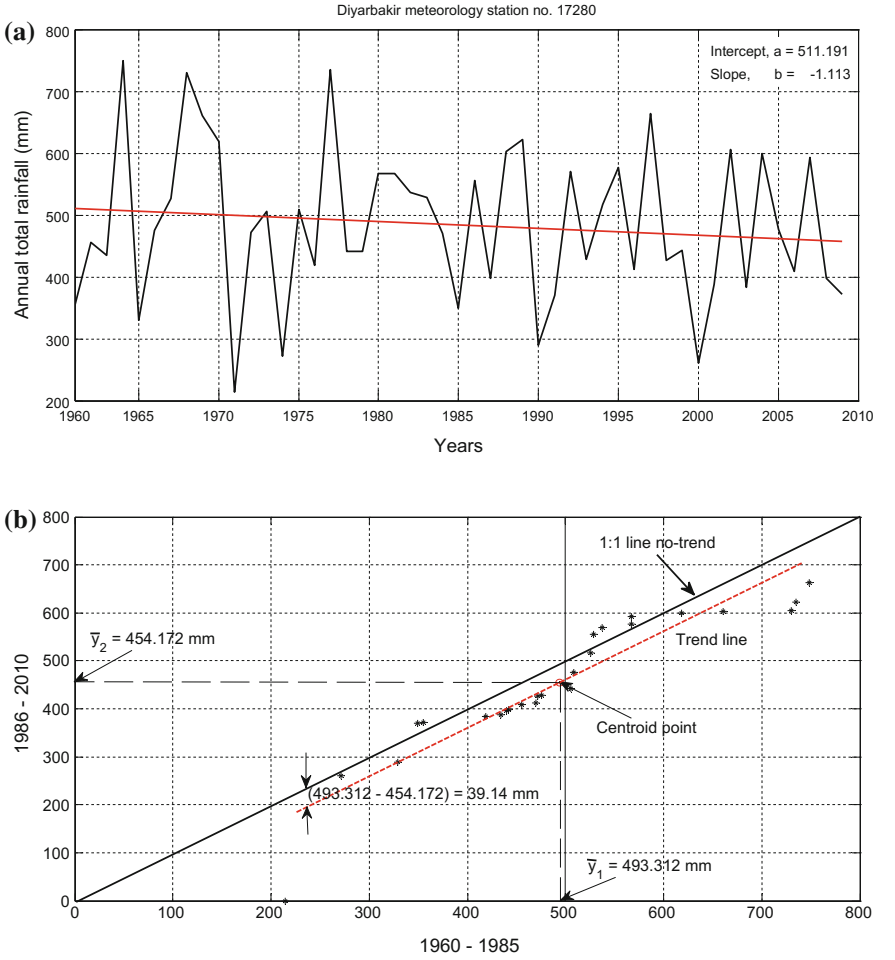

Fig. 5.28 Diyarbakir meteorology station annual total rainfall data. **a** Time series and trend, **b** innovative trend plot

station rainfall records at Diyarbakir meteorology station in the Southeastern part of Turkey. The suggested methodology is easy to apply and all the steps are logically presented in a rational manner.

Table 5.3 Innovative trend test results

No.	Name of stations	New Jersey	Danube River	Diyarbakir	Operations
1	Type of data	Annual temperature (°F)	Annual discharge (m^3/s)	Annual total rainfall (mm)	
2	Number of data	116	164	49	
3	Slope, b	0.021	−0.587	−1.113	Equation (5.3)
4	Intercept, a	51.818	5614.94	511.191	Equation (5.6)
5	Standard dev., σ	1.3025	944.921	124.738	From the whole series, y
6	Correlation, $\rho_{\bar{y}_1\bar{y}_2}$	0.9749	0.9767	0.9495	Ordered half series cross-correlations
7	Slope standard dev., σ_b	0.000467	0.1942	0.2386	Equation (5.10)
8	Significance level	0.05	0.05	0.05	Practically adopted
9	Lower CL	−0.000768	−0.3194	−0.3925	Equation (5.11)
10	Upper CL	+0.000768	+0.3194	+0.3925	Equation (5.11)
11	Hypothesis	H_a	H_a	H_a	Alternative hypothesis
12	Decision	Yes	Yes	Yes	According to H_a
13	Type of trend	Increasing	Decreasing	Decreasing	According to sign of b

5.6 Crossing Trend Analysis Methodology

Trend analyses are the necessary tools for depicting possible general increase or decrease in a given hydro-climatologic time series. There are many versions of trend identification methodologies such as the M–K trend test, S-R, Sen's slope, regression line, and Şen's innovative trend analysis. The literature has many papers about the use, cons and pros, and comparisons of these methodologies. In this section, a completely new approach is proposed based on the crossing properties of a time series. It is suggested that the suitable trend from the centroid of the given time series should have the maximum number of crossings (total number of up-crossings or down-crossings). This approach is applicable whether the time series has dependent or independent structure and also without any dependence on the type of the probability distribution function. The validity of this method is presented through extensive Monte Carlo simulation technique and its comparison with other existing trend identification methodologies.

Trend identification is one of the major topics in data processing concerning social, medical, industrial, scientific, and engineering studies for betterment of future predictions. Their physical causes maybe due to the changes in the natural events such as the climate change or depreciation and improvement in the human made instruments. Especially, in water sciences increasing and decreasing trend

tendencies bring into consideration the assessments of droughts, water scarcities, desertifications or floods and flash floods with water inundations. These water related events are also reflective in the agricultural and food production sectors. Climate change due to global warming has huge impact on the environment, weather patterns, and rise in sea level, which can be depicted by temporal trend analysis.

Although the visual appreciation of trend component in a given hydro-climatologic time series has been possible since the start of meteorological records in the second part of the eighteenth century, development of analytical methodologies came into existence in the first part of the nineteenth century (Mann 1945). His method provides information whether there is a trend within the time series with its verbal direction as increasing, decreasing, or neutral type. Later, Sen (1968) provided a quantitative slope calculation method for the trend component within a given time series. The M–K nonparametric trend test (Mann 1945), is functionally identical to Kendall's (tau) test for correlation (Kendall 1975), and the associated slope estimation by Sen (1968) median procedure.

On the other hand, Spearman's rho, which is a distribution-free statistic, is useful for the trend significance test (Spearman 1904). It is less widespread than the commonly applicable M–K trend test. However, the two tests are equivalent for the case of serially independent observations. Daniel (1990) has provided further explanations and improvements in the application of the Spearman's tau approach.

The regression monotonic line is among the parametric procedures for trend testing. The two sample t-test can be applied for step type of trends (Iman and Conover 1983). In these procedures, trend magnitude estimations are the regression slope and the difference in the means. On the other hand, nonparametric methods are the Mann–Kendall test and the Rank-Sum test (Bradley 1968), and their trend estimations are obtained according to Sen (1968), which is equivalent to the median of all pairwise slopes in the data set. Additionally, the Hodges–Lehmann estimator is the median of all differences between data in the first data set and data in the second data set (Hodges and Lehmann 1963).

Nonparametric procedures have significantly higher power than parametric procedures in cases of substantial departures from normal (Gaussian) probability distribution function (PDF) and the large sample sizes (Helsel and Hirsch 1988).

In addition to all available trend methodologies, a new one is suggested in this chapter as the "crossing trend," which depends on the maximum number of crossings (up-crossings or down-crossing) within a given hydro-climatological time series. This method hypothesis a set of different slope trends and the one with the maximum-crossing point is identified as the valid one.

The main purpose of this chapter is to suggest an innovative crossing trend analysis methodology with its significance test. The validity of this method is confirmed by extensive Monte Carlo simulation technique by taking into consideration different sample sizes and probability distribution functions (PDFs). The results are compared with the Sen's slope method and it is found that the differences are within the practically acceptable relative error percentage of $\pm 10\%$. The application of the innovative crossing trend analysis is performed for actual

meteorological records of annual daily extreme (maximum) rainfall from seven different climatological regions of Turkey.

5.6.1 Rational Concept

The main idea is that at various trend slope truncation levels that passes through the time series centroid, the number of crossing (up-crossings or down-crossings) is the maximum (Şen 2017). In order to illustrate this point, a hypothetical time series and its truncation—at different trend levels are given with the number of crossing points in Fig. 5.29.

In this figure, a series of increasing and decreasing trends are given and among them the one with the maximum crossing (up-crossing or down-crossing) number is the most representative trend-line. In this manner, the trend identification does not depend on the PDF of the hydro-climatologic variable. Besides, one can also calculate the surplus and deficit quantities on the basis of the trend line, if necessary. In Fig. 5.30, various quantities along the truncation level are shown. In this figure, SL (DL) implies surplus (deficit) lengths and there are 5(4) of them.

5.6.2 Theoretical Background

In any hydro-climatologic record series-crossing points at a truncation level provide not only information on wet and dry spell features, but also about the internal structure of the series (Şen 1977). For instance, the more is the crossing points at the median truncation level, the less is the serial dependence. In an independent series at the median level practically the number of up-crossings is equal to the

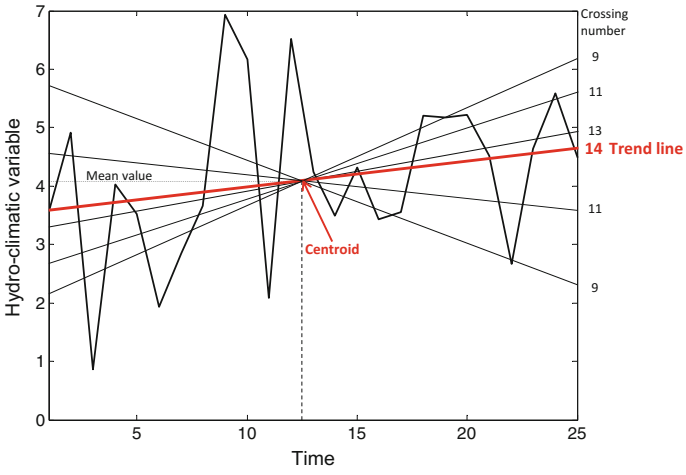

Fig. 5.29 Time series and trend crossing numbers

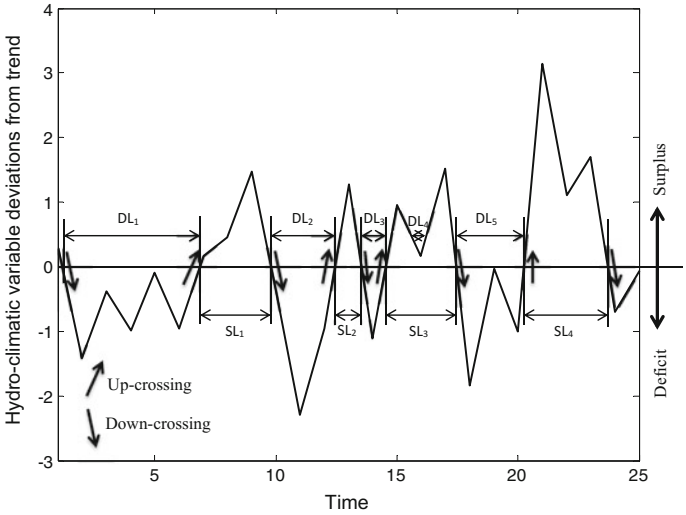

Fig. 5.30 Truncation (trend) level features

down-crossing number. In Fig. 5.30, up-crossings and down-crossings are indicated with arrows. Theoretically, in an infinite independent series, irrespective of the PDF, the number of crossings abide by the Poisson process (Feller 1968). However, in finite sample lengths, n, the expectation and the variance of the number of up-crossings, N_u, have been derived by Şen (1991) as

$$E(N_u) = np(1-p) \tag{5.12}$$

and

$$V(N_u) = E(N_u)\left(1 - 3p + 3p^2\right), \tag{5.13}$$

respectively. Herein, p is the probability of surplus numbers over the median truncation level. The average number of up-crossings increases with the sample length, n, but decreases as the truncation level increases. The maximum up-crossing (down-crossing) number occurs at 0.5 truncation level (Fig. 5.31). In general, such a truncation level corresponds to average = mode = median value in symmetrical PDFs, but to the median value in unsymmetrical PDFs (Fig. 5.31).

The PDF of up-crossings is shown to be in accord with the normal (Gaussian) PDF with mean and variance as in Eqs. (5.12) and (5.13), respectively. The standard deviation of the up-crossing number is shown in Fig. 5.32.

Under the light of the aforementioned information, it is possible to benefit from a normal (Gaussian) PDF for the significance test of innovative crossing trend either by the use of Eqs. (5.12) and (5.13) or with their standardization as

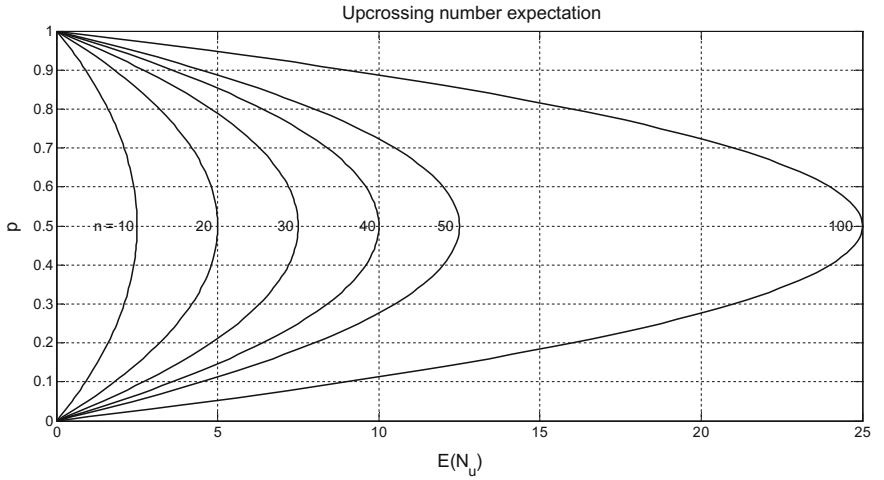

Fig. 5.31 Up-crossing number expectations for a set of sample lengths

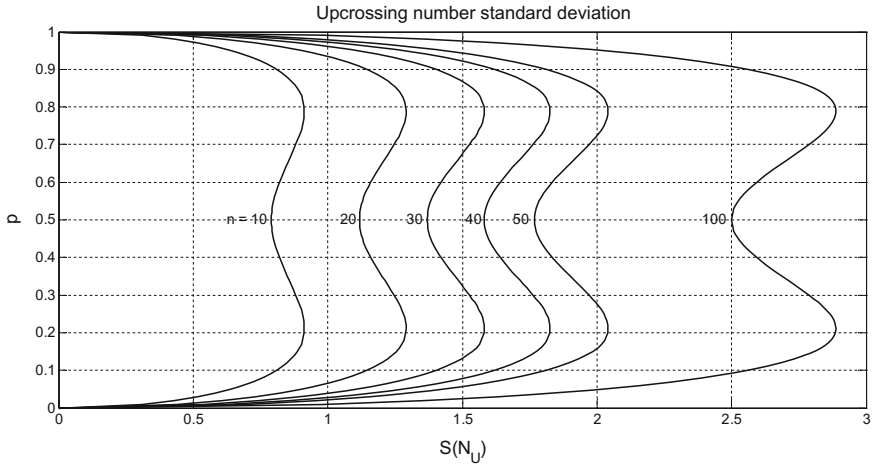

Fig. 5.32 Up-crossing number standard deviation for a set of sample lengths

$$m_s = \frac{E(N_u)}{n(n-1)} \tag{5.14}$$

and

$$s_s = \frac{V(N_u)}{E(N_u)(1-3p-3p^2)} \tag{5.15}$$

respectively.

5.6.3 Monte Carlo Simulations

In order to fix the validity of the crossing trend analysis, a set of Monte Carlo simulation studies is achieved, where 1,000 synthetic series are generated according to normal (Gaussian), Gamma and exponential PDF's. Each synthetic series is subjected to suggested innovative crossing trend analysis, the Mann–Kendall trend test, Sen's slope and Şen (2012, 2014) innovative trend slope and corresponding trend lines. In the simulations, the set of embedded slopes, s_d, are considered as decreasing (increasing) trends −0.007, −0.005, −0.003, −0.001 (0.1, 0.3, 0.5 and 0.7) with sample sizes as 25, 50, and 100. The simulation results are given as a set of graphs in Fig. 5.33. In this figure for each PDF three graphs are shown for the sake of visual inspection each for sample sizes 25, 50, and 100.

The numerical results of extensive simulation study are presented in Table 5.4. The simulations are carried on for three PDFs, namely standard normal (Gaussian) PDF with zero mean and unit standard deviation; Gamma PDF with location and scale parameters as 2 and 1, respectively; finally, the exponential PDF with its single parameter as 2.

Both Gamma and exponential PDF generations can be achieved with different parameter sets, but for the sake of brief description in this chapter only the aforementioned parameters are considered.

In this table, n indicates the sample length and R.E. is defined as the absolute relative error

$$\text{R.E.} = 100\frac{|s_e - s_c|}{s_e}, \tag{5.16}$$

where s_e and s_s are embedded and innovative crossing trend simulation slopes, respectively. In the first column of Table 5.1 are the embedded slope values, and simulation trend slopes are shown in the second, fourth, and the sixth columns under each sample length. It is obvious from this table that the absolute relative errors are less than practically acceptable 10% level, and the mean R.E. values are far less that this acceptable percentage level.

After all what have been explained so far as the simulation results are concern, it is evident that the innovative crossing trend analysis is valid for practical applications.

5.6.4 Application

For the application of the innovative crossing trend analysis, seven annual daily extreme rainfall records are considered from seven different climatology regions of Turkey. Each one has more than 50 years of records and this is a statistically valid sample size for reliable studies. The meteorology station locations are given in Fig. 5.34.

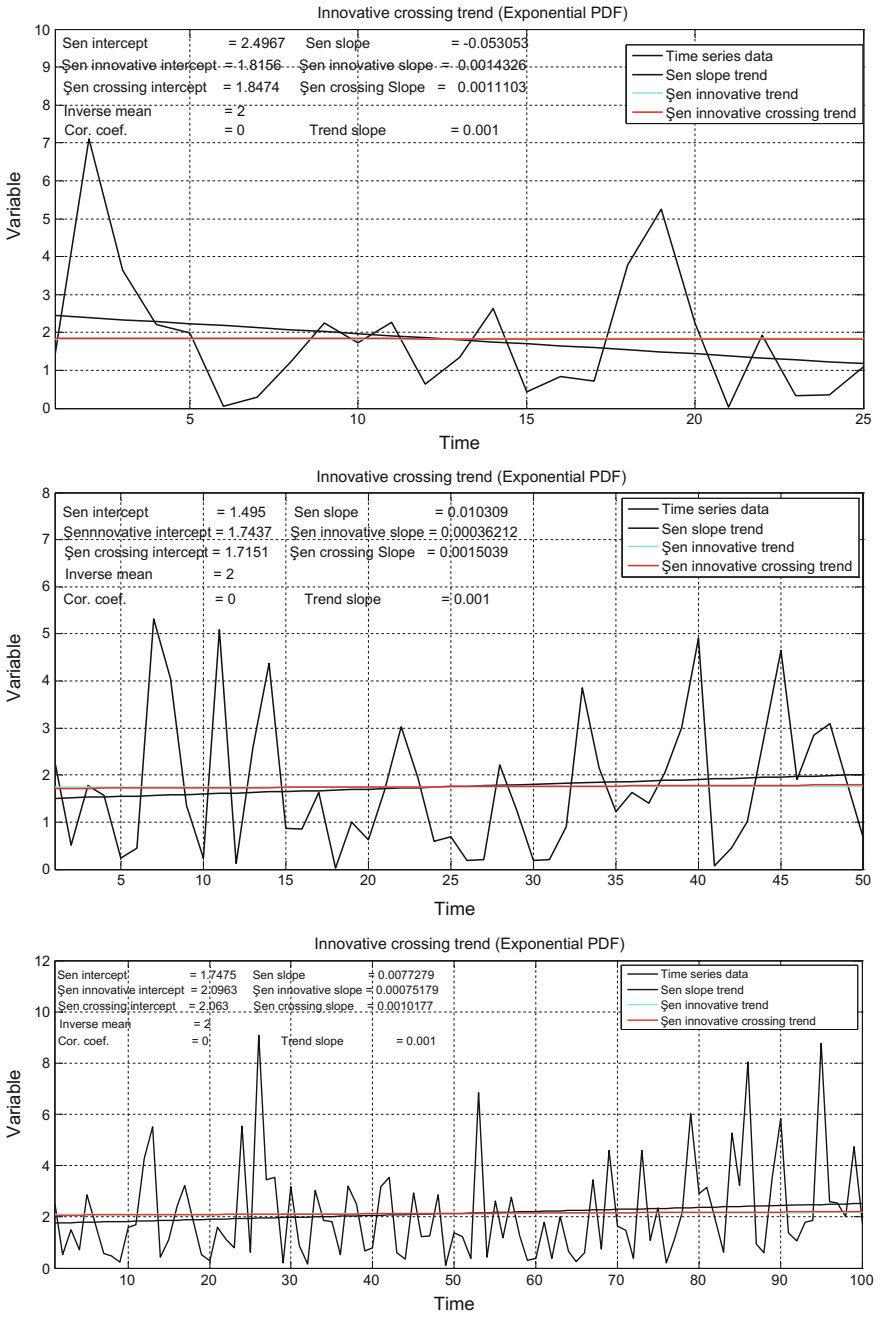

Fig. 5.33 PDF simulation results

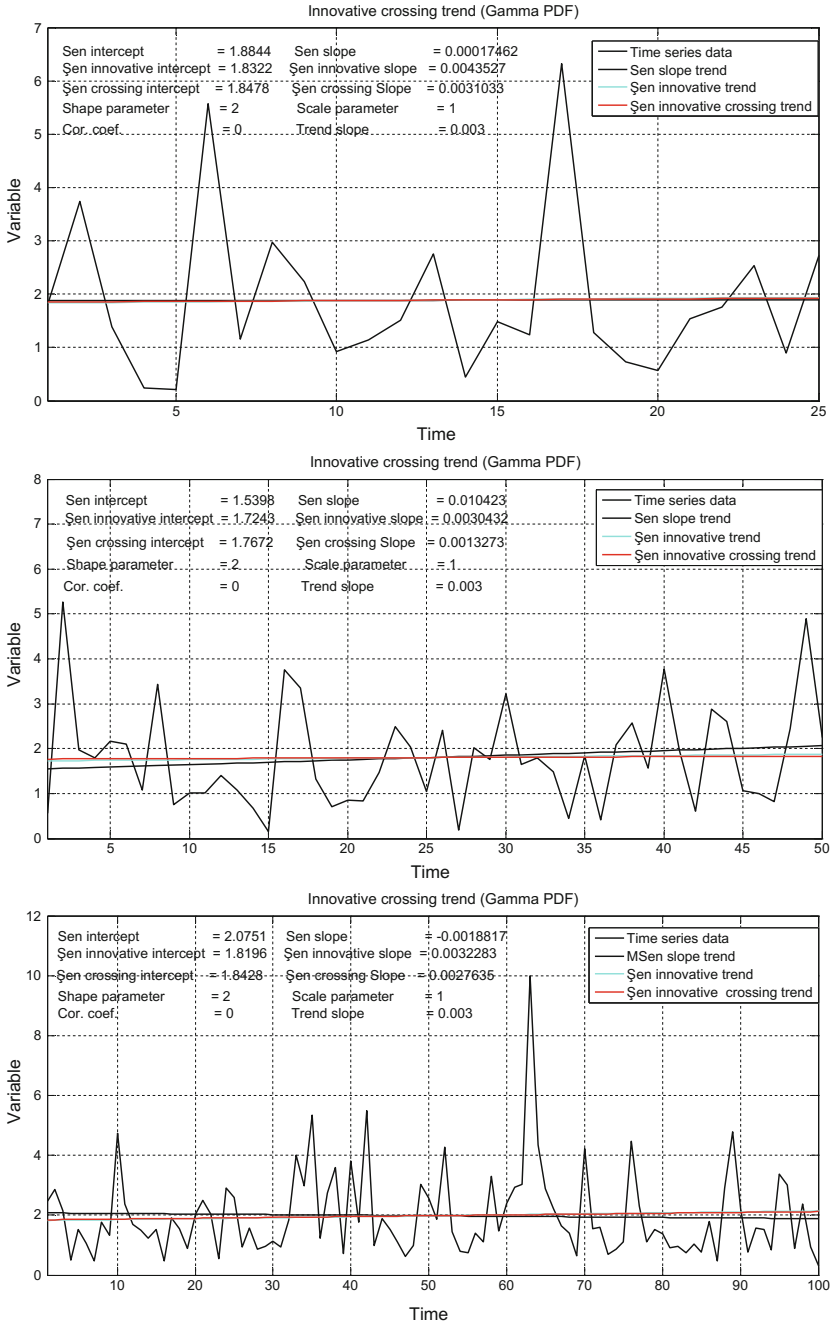

Fig. 5.33 (continued)

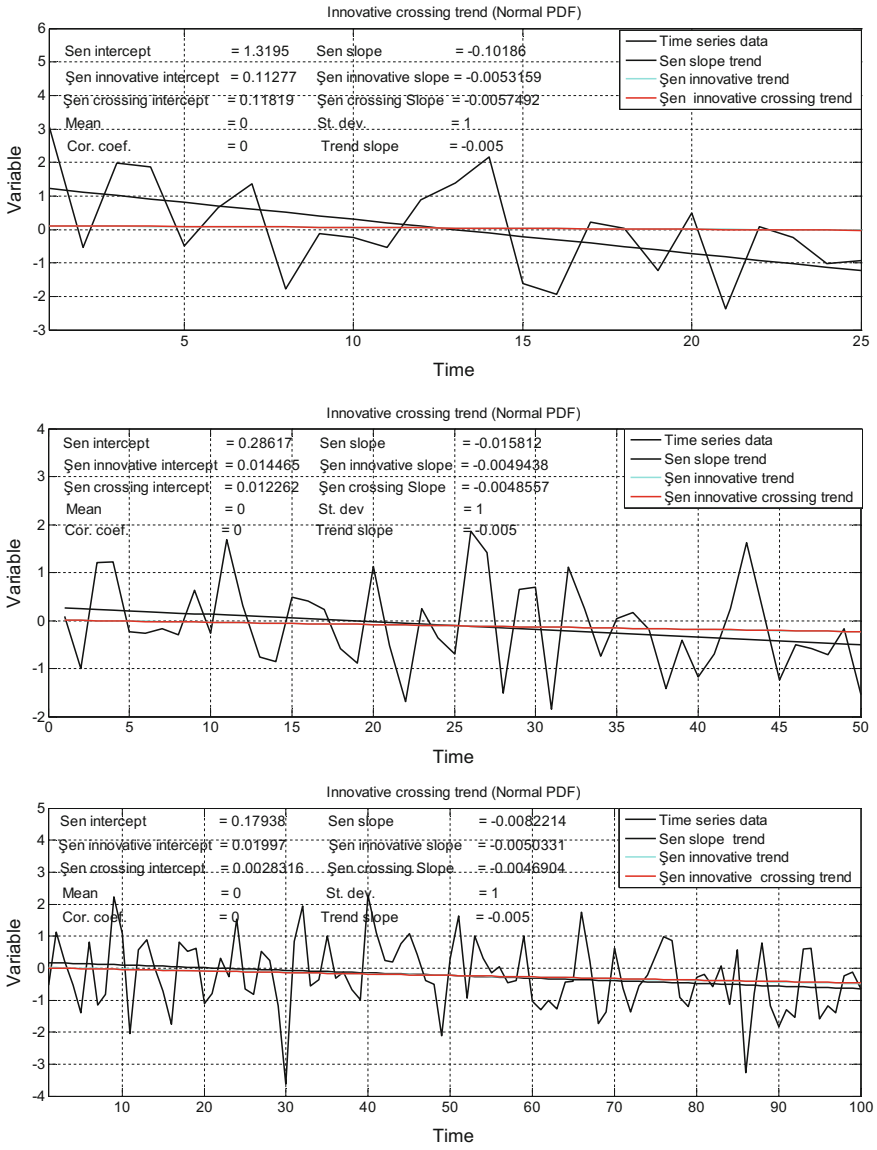

Fig. 5.33 (continued)

Each station represents different climatological region within Turkey. For instance, Ankara station is located in a dry, rather arid, and steppic region in the Central Anatolia, which is far away from the maritime climatic effects. This area includes the least rainfall receiving region of Turkey with annual average rainfall amounts less than 250 mm. Antalya is located along the Mediterranean coastal area of Turkey with typical Mediterranean climate impacts. Toward the northern part of

Table 5.4 Simulation results with relative error percentages

Gaussian PDF						
Embedded slope, s_e	n = 100	R.E. (%)	n = 50	R.E. (%)	n = 25	R.E. (%)
0.0010	0.0011	9.1000	0.0011	9.0909	0.0011	9.7473
0.0030	0.0033	9.7667	0.0033	9.6386	0.0027	9.4092
0.0050	0.0054	8.5400	0.0051	1.5748	0.0057	12.0338
0.0070	0.0072	2.3000	0.0066	5.3107	0.0078	10.6345
−0.0070	−0.0076	8.8857	−0.0075	6.1788	−0.0073	3.5015
−0.0050	−0.0047	6.2000	−0.0049	2.9442	−0.0057	11.4888
−0.0030	−0.0032	6.8000	−0.0032	6.9479	−0.0033	9.0909
−0.0010	−0.0011	10.3000	−0.0011	9.0082	−0.0010	2.2495
Mean	–	7.7365	–	6.3368	–	8.5194
Gamma PDF						
0.0010	0.0009	5.4852	0.0010	3.1946	0.0011	5.6604
0.0030	0.0028	8.5384	0.0030	1.4131	0.0031	3.3194
0.0050	0.0050	0.9285	0.0054	7.4417	0.0045	10.6440
0.0070	0.0068	2.3691	0.0073	3.7801	0.0067	4.0583
−0.0070	−0.0073	3.8065	−0.0078	10.4859	−0.0079	10.9641
−0.0050	−0.0051	2.2101	−0.0050	0.1201	−0.0049	1.9992
−0.0030	−0.0031	4.0307	−0.0032	5.2133	−0.0032	7.0344
−0.0010	−0.0009	6.6098	−0.0011	9.5841	−0.0011	9.0909
Mean	–	4.2473	–	5.1541	–	6.5963
Exponential PDF						
0.0010	0.0010	1.7682	0.0011	9.4203	0.0009	9.2896
0.0030	0.0031	1.9287	0.0033	10.1527	0.0033	9.1460
0.0050	0.0049	2.2077	0.0048	4.3841	0.0050	0.8723
0.0070	0.0077	9.5490	0.0074	4.9946	0.0078	10.1873
−0.0070	−0.0071	1.9471	−0.0076	8.3170	−0.0077	9.2912
−0.0050	−0.0054	6.5246	−0.0048	4.6025	−0.0047	6.8148
−0.0030	−0.0031	3.8770	−0.0028	6.8376	−0.0033	8.2849
−0.0010	−0.0011	7.1495	−0.0011	9.9099	−0.0011	9.4203
Mean	–	4.3690	–	7.3273	–	7.9133

this region are the Taurus Mountain chain with elevations more than 3,000 m above mean sea level, and therefore, it is one of the humid regions in Turkey. Frequent orographic rainfall types occur, which causes to occasional floods. The geological composition is of limestone and dolomatic rocks with karstic features, and therefore, rainfalls recharge the groundwater in the region. It is regarded as one of the surface and ground water rich parts of Turkey. Diyarbakir station is in the

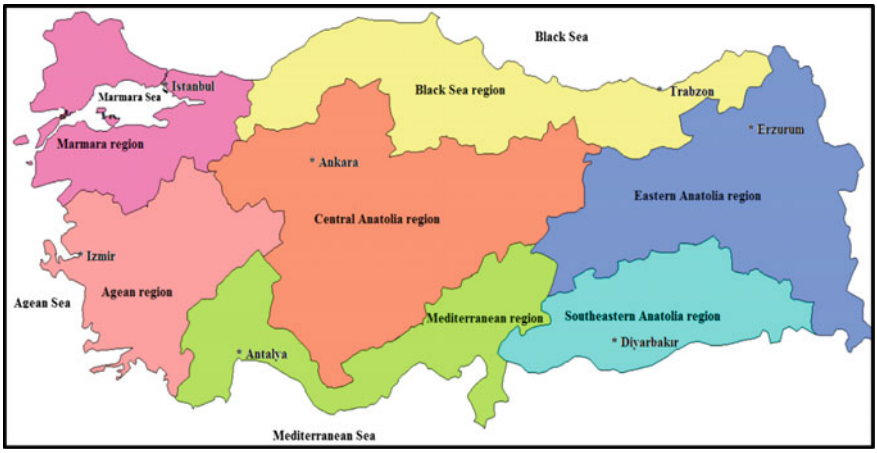

Fig. 5.34 Meteorology station locations

southeastern province of Turkey away from the sea born air mass movements, and therefore, it has continental climatic features. Due to its unique position at the upper end of the Mesopotamian valley, the rainfall occurrences are rare and mostly summer seasons are extremely hot and winter seasons are mild. Erzurum station represents rugged mountainous region of eastern Turkey with severe winter conditions and rather cool summer months. Izmir location is the representative of the Aegean Sea at the western coastal area of Turkey. It has hot summer months and mild winter season with moderate rainfall events throughout the year. Finally, Trabzon meteorology station is chosen for the representation of the Black Sea rainfall regime, which is rainy almost throughout the year. This is due to the fact that North Atlantic born air masses that descend southwesterly over the Europe and then over the Black Sea with moisture and the coastal parallel mountain chains cause to frequent orographic and cyclonic rainfall occurrences.

Seven meteorology station records are treated by the innovative crossing trend analysis and also classical Sen's slope regressions. Figure 5.35 indicates the innovative crossing trends in each record and also the test results are presented in Table 5.6 for each station by considering the Sen slope and the suggested methodology features as explained in Sects. 5.6.1 and 5.6.2.

Visual inspection of each graph provides reflections that the innovative crossing trend analysis well identifies the trend component in each location. For the sake of comparison trend calculated on the basis of Sen's slope is also given on the same graphs.

However, for quantitative analyses Table 5.6 is prepared, where both Mann–Kendall trend test and the innovative crossing trend analysis quantities are presented. In this table LL and UL are for the lower and upper significance levels. It is

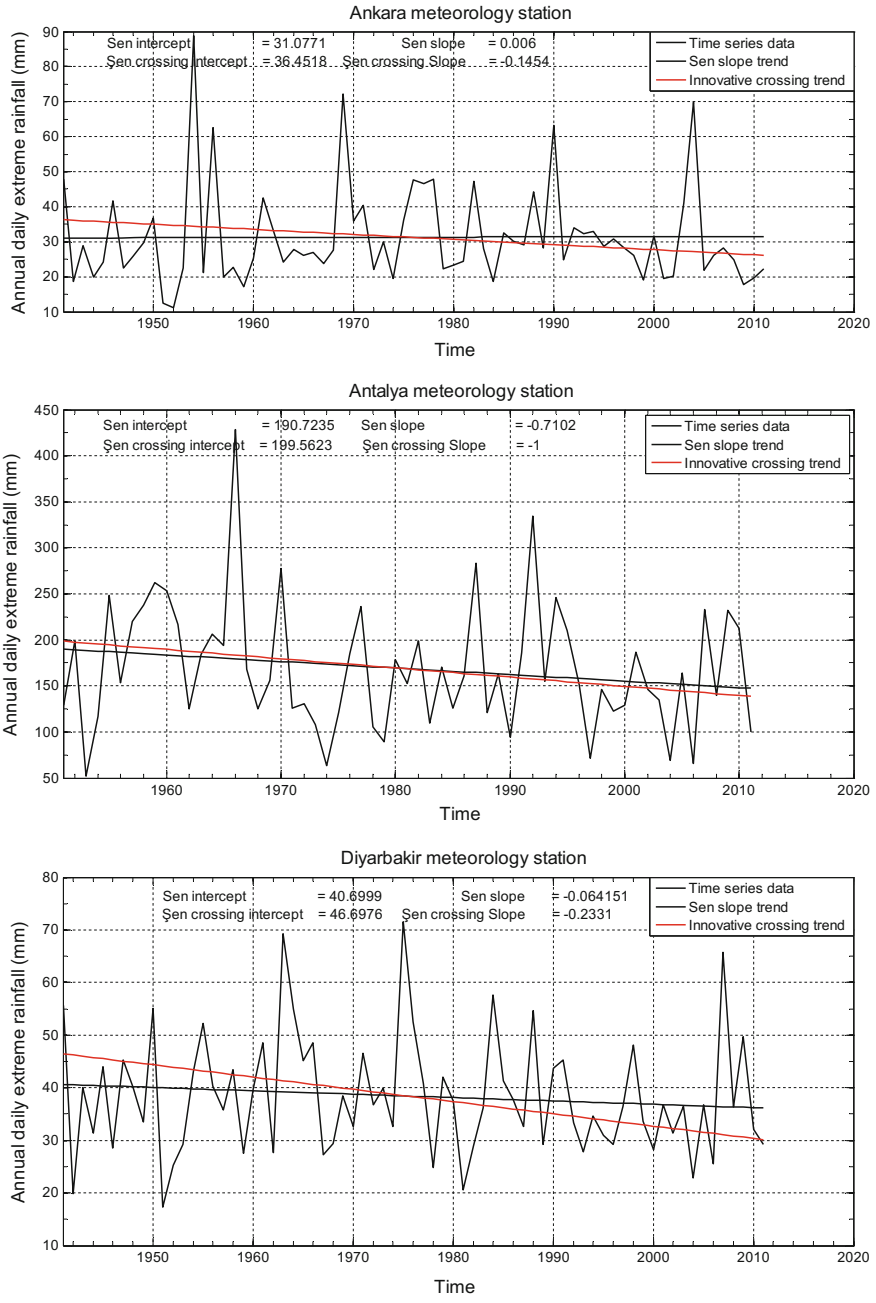

Fig. 5.35 Innovative crossing trend components

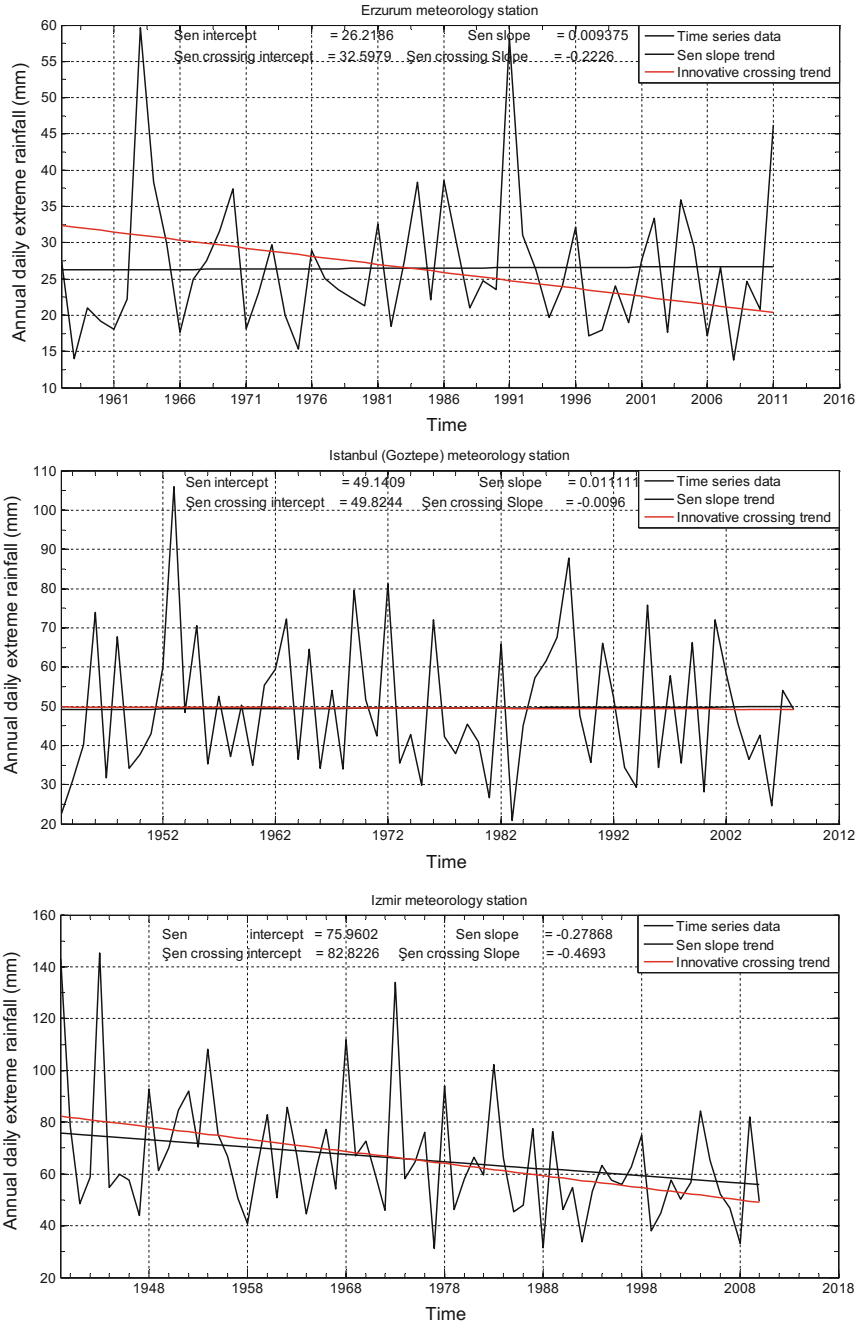

Fig. 5.35 (continued)

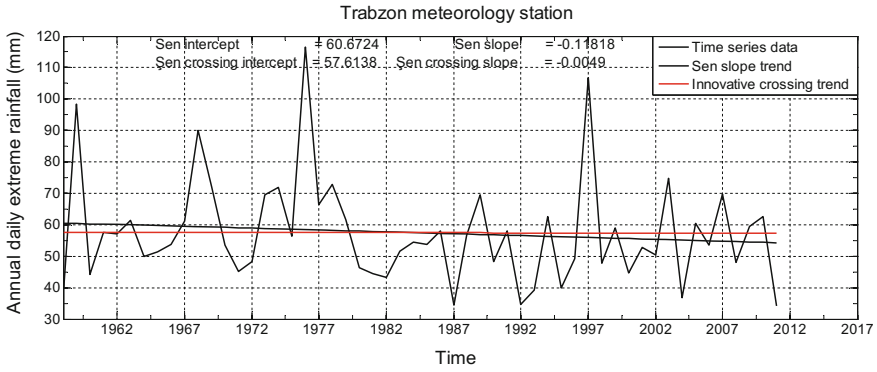

Fig. 5.35 (continued)

to be noticed that the confidence limits in the case of Mann–Kendall trend test remain the same without depending on the sample size. However, as obvious from Eqs. (5.14) and (5.15) the confidence limits are functions of the sample size for the innovative crossing trend analysis. Z is the statistics value of the Mann–Kendall trend test, and C is the number of up-crossing for the innovative crossing trend calculations. In the table, trend tests are probed for two levels, 90 and 95%.

Trend component identification in the climatological time series constitutes very important aspect, especially for the climate change description and, therefore, such studies have increased unprecedentedly since the last three decades. There are different methodologies for this purpose, but each one with restrictive assumptions. In this chapter, entirely new concept of trend identification is proposed by taking into consideration the number of crossings on the possible trend line. It is stated that the trend component should have the maximum number of crossings among many different trend alternatives. In order to select the most valid one, the given climatological time series is probed with a set of trend representatives that passes through the centroid point of the data. The centroid is defined as the point in the time series with abcissa as the half of the sample size and the ordinate equal to the median of the recorded values. The formulations are given at the median level as for the number and the variance of the crossing points with no trend within a serially independent time series. They do not dependent on the type of probability distribution function. The validity of innovative crossing approach is shown by extensive Monte Carlo simulation studies based on different sample sizes and probability distribution functions. The application of the innovative up-crossing trend analysis is presented for seven distinctive climatological regions of Turkey for annual daily extreme (maximum) rainfall records, which have physically independent serial structure so as to abide with the theoretical requirement of the suggested methodology.

Table 5.6 Mann−Kendal and innovative crossing trend statistical characteristics

95% confidence								
	Mann–Kendall			Decision	Innovative crossing			Decision
	LL	Z	UL		LL	C	UL	
Ankara	−1.6449	0.1191	1.6449	No significance	−21.2149	15.5	21.2149	No significance
Antalya	−1.6449	−1.2944	1.6449	No significance	−18.4617	17	18.4617	No significance
Diyarbakir	−1.6449	−0.9778	1.6449	No significance	−21.2149	21.5	21.2149	Significant trend
Erzurum	−1.6449	0.1307	1.6449	No significance	−16.7996	16	16.7996	No significant trend
Istanbul	−1.6449	0.1771	1.6449	No significance	−19.8407	21.5	19.8407	Significant trend
Izmir	−1.6449	−2.5959	1.6449	Significant trend	−21.4893	19.5	21.4893	No significant trend
Trabzon	−1.6449	−0.843	1.6449	No significance	−16.5218	16	15.5218	No significance
90% confidence								
Ankara	−1.2816	0.1191	1.2816	No significance	−20.4496	15.5	20.4496	No significance
Antalya	−1.2816	−1.2944	1.2816	Significant	−17.7523	17	17.7523	No significance
Diyarbakir	−1.2816	−0.9778	1.2816	No significance	−20.4496	21.5	20.4496	Significant
Erzurum	−1.2816	0.1307	1.2816	No significance	−16.1261	16	16.1261	No significance
Istanbul	−1.2816	0.1771	1.2816	No significance	−19.1028	21.5	19.1028	Significant
Izmir	−1.2816	−2.5959	1.2816	Significant	−20.7186	19.5	20.7186	No significance
Trabzon	−1.2816	−0.843	1.2816	No significance	−15.8544	16	15.8544	Significant

References

Barbosa, S. M., Silva, M. E., & Fernandes, M. J. (2008). Time series analysis of sea-level records: Characterizing long-term variability. In R. V. Donner & S. M. Barbosa (Eds.), *Nonlinear time series analysis in the geosciences—applications in climatology, geodynamics, and solar-terrestrial physics* (pp. 157–173). Berlin: Springer.

Box, G. E. P., & Jenkins, G. M. (1970). *Time series analysis*. Holden-Day, San Francisco, CA: Forecasting and Control.

Bradley, J. V. (1968). *Distribution-free statistical tests*. Englewood Cliffs, N.J: Prentice-Hall.

Brunetti, M., Colacino, M., Maugeri, M., & Nanni, T. (2001). Trends in the daily intensity of precipitation in Italy from 1951 to 1996. *International Journal of Climatology, 21,* 299–316.

Burn, D., Mohamed, A., & Elnur, H. (2002). Detection of hydrologic trends and variability. *Journal of Hydrology, 255,* 107–122.

Daniel, D. (1990). Summary review of construction quality control for earthen liners. In R. Bonaparte (Ed.), *Waste Containment Systems: Construction, Regulation, and Performance* (pp. 175–189), GSP No. 26, ASCE.

Douglas, E. M., Vogel, R. M., & Kroll, C. N. (2000). Trends in floods and low flows in the United States: Impact of spatial correlation. *Journal of Hydrology, 240,* 90–105.

Feller, W. (1968). *An introduction to probability theory and its applications* (Vol. I, 3rd ed.). Wiley.

Groisman, P. Y., Knight, R. W., & Karl, T. R. (2001). Heavy precipitation and high streamflow in the contiguous United States: Trends in the 20th century. *Bulletin of the American Meteorological Society, 82,* 219–246.

Groisman, P. Y., Knight, R. W., Karl, T. R., Easterling, D. R., Sun, B., & Lawrimore, J. H. (2004). Contemporary changes of the hydrological cycle over the contiguous United States: Trends derived from in situ observations. *Journal of Hydrometeorology, 5*(1), 64–85.

Hazen, A. (1914). Storage to be provided in impounding reservoirs for municipal water supply. *Transactions of the American Society of Civil Engineers, 77,* 1308.

Helsel, D. R., & Hirsch, R. M. (1988). Discussion of "applicability of the t-test for detecting trends in water quality variables" by R.H. Montgomery and J.C. Loftis. *Water Resources Bulletin, 24,* 201–204.

Hirsch, R. M., & Slack, J. R. (1984). A nonparametric trend test for seasonal data with serial dependence. *Water Resources Research, 20*(1), 727–732.

Hodges, J. L., Jr., & Lehmann, E. L. (1963). Estimates of location based on rank tests. *The Annals of Mathematical Statistics, 34,* 598–611.

Iman, R. L., & Conover, W. J. (1983). *A modern approach to statistics*. New York: Wiley.

Intergovernmental Panel on Climate Change (IPCC). (2007). *Climate change 2007: The physical science basis. contribution of working group i to the fourth assessment report of the intergovernmental panel on climate change*. New York: Cambridge University Press.

Kahya, E., & Kalaycı, S. (2004). Trend analysis of stream flow in Turkey. *Journal of Hydrology, 289,* 128–144.

Kalra, A., Piechota, T. C., Davies, R., & Tootle, G. A. (2008). Changes in U.S. streamflow and western U.S. snowpack. *Journal of Hydrologic Engineering, 13,* 156–163.

Kendall, M. G. (1975). *Rank correlation methods*. New York: Oxford University Press.

Lettenmaier, D. P., Anderson, D., & Brenner, R. (1984). Consolidation of a stream quality monitoring network.*Water Resources Bulletin, 20*(4), 473–481.

Lettenmaier, D. P., Wood, E. F., & Wallis, J. R. (1994). Hydroclimatological trends in the continental United States, 1948–88. *Journal of Climate, 7,* 586–607.

Lins, H. F., & Slack, J. R. (1999). Streamflow trends in the United States. *Geophysical Reseach Letters, 26*(2), 227–230.

Mann, H. B. (1945). Nonparametric tests against trend. *Econometrica, 13,* 245–259.

McCabe, G. J., & Wolock, D. M. (2002). A step increase in streamflow in the conterminous United States. *Geophysical Reseach Letters, 29*(24), 2185.

Miller, W. P., & Piechota, T. C. (2008). Regional analysis of trend and step changes observed in hydroclimatic variables around the Colorado River Basin. *Journal of Hydrometeorology, 9*(5), 1020–1034.

Montanari, M., Rosso, R., & Taqqu, M. S. (1997). Fractionally differenced ARIMA models.

Sen, P. K. (1968). Estimates of the regression coefficient based on Kendall's Tau. *Journal of American Statistical Association, 63,* 1379–1389.

Şen, Z. (1974). Small sample properties of stationary stochastic processes and the hurst phenomenon in hydrology. unpublished Ph. D. Thesis, Imperial College of Science and Technology, University of London, 256p.

Sen, P. K. (1978). Estimates of the regression coefficient based on Kendall's Tau. *Journal of American Statistical Association, 63,* 1379–1389.

Şen, Z. (1977). Autorun analysis of hydrologic time series. *Journal of Hydrology, 36,* 75–85.

Şen, Z. (1991). Probabilistic modelling of crossing in small samples and application of runs to hydrology. *Journal of Hydrology, 124*(3–4), 345–362.

Şen, Z. (2012). Innovative trend analysis methodology. *Journal of Hydrologic Engineering, 17*(9), 1042–1046.

Şen, Z. (2014). Trend identification simulation and application. *Journal of Hydrologic Engineering, 19,* 241–245.

Şen, Z. (2017). Innovative crossing trend analysis and application. *Theoretical and Applied Climatology* (in print).

Spearman, C. (1904). The proof and measurement of association between two things. *American Journal of Psychology, 15*, 72–101.

Trenberth, K. E., et al. (2007). *Observations: Surface and atmospheric climate change, in climate change 2007: The physical science basis. contribution of working group i to the fourth assessment report of the intergovernmental panel on climate change, chap. 3*. New York: Cambridge University Press.

Wang, Y., & Zhou, L. (2005). Observed trends in extreme precipitation events in China during 1961–2001 and the associated changes in large-scale circulation. *Geophysical Reseach Letters, 32,* L09707. doi:10.1029/2006GL022574.

Xiong, L. H., and Guo, S. L. (2004). Trend test and change-point detection for the annual discharge series of the Yangtze River at the Yichang hydrological station. *Hydrological Sciences Journal, 49*(1), 99–112.

Yue, S., Pilon, P., & Cavadia, G. (2002a). Corrigendum to "Power of the Mann-Kendall and Spearman's rho tests for detecting monotonic trends in hydrological series". *Journal of Hydrology, 259,* 254–271.

Yue, S., Pilon, P., & Cavadia, G. (2002b). Corrigendum to "Power of the Mann-Kendall and Spearman's rho tests for detecting monotonic trends in hydrological series". *Journal of Hydrology, 259,* 254–271.

Yue, S., Pilon, P., Phinney, B., & Cavadias, G. (2002c). The influence of autocorrelation on the ability to detect trend in hydrological series. *Hydrological Processes, 16*, 1807–1829.

Zhang, X., Harvey, K. D., Hogg, W. D., & Yuzyk, T. R. (2001). Trends in Canadian streamflow. *Water Resources Research, 37,* 987–998.